ACS Sensors, Available online 7 July 2026
DOI: 10.1021/acssensors.6c00719

Paper microfluidic platform using multiplexed isothermal amplification and CRISPR/Cas12a for aquatic pathogen detection

Yuwei Pan[1, 2], Zhugen Yang[1, *]

[1]Faculty of Engineering and Applied Sciences, Cranfield University, Cranfield, MK43 0AL, UK

[2]College of Chemical and Biological Engineering, Zhejiang University, Hangzhou, 310058, China

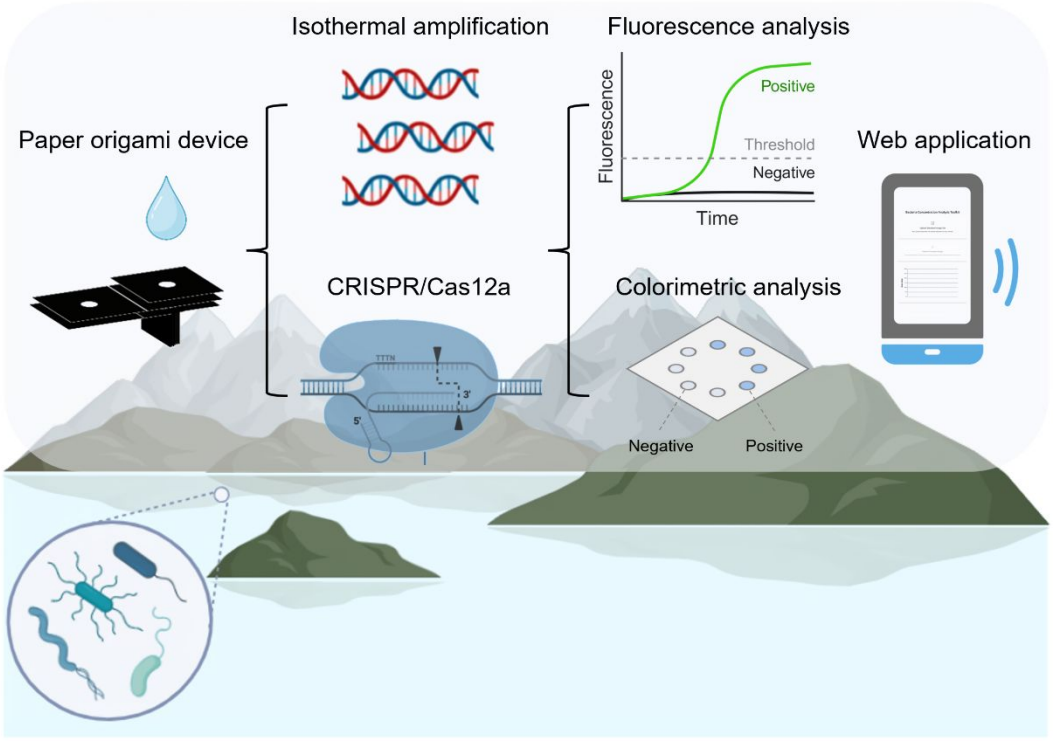
*Corresponding author: Zhugen Yang (zhugen.yang@cranfield.ac.uk)

Abstract: The global health threat posed by microbial contamination of aquatic systems demands feasible pathogen monitoring solutions. However, current detection methods are limited by expensive instrumentation and specialized personnel, which hinders their application in point-of-care testing (POCT). Here we presented an integrated paper microfluidic platform for spatially multiplexed detection of pathogenic bacteria, including *Salmonella*, *E. coli*, *C. perfringens*, *B. cereus*, *V. parahaemolyticus*, *S. aureus*, and *L. monocytogenes*, selected due to their epidemiological significance and regulatory relevance in environmental and food safety monitoring. LAMP, RAA-CRISPR, and RPA-CRISPR assays were housed within physically isolated reaction chambers on two-layer chips. An engineered horseradish peroxidase (HRP) cascade-coupled crRNA modification system with DNA-conjugated labels was designed for colorimetric detection. Operation was enabled by solar-powered and portable hardware for incubation and imaging, coupled with web application for quantitative analysis. Exceptional analytical performance was demonstrated, achieving a LOD of 1 CFU/mL, a dynamic range of 1–10^7 CFU/mL, high reproducibility (CV < 5%), low batch-to-batch variation (< 6%), low cost (£2.5 per test), and scalable integration, with a sample-to-answer time of 60 min. Successful field validation in diverse aquatic environments confirmed its practical feasibility, consistent with gold standard PCR (R^2 = 0.98). This platform offers a promising POCT solution for public health protection and epidemic monitoring, particularly in resource-limited settings.

Keywords: Paper microfluidic platform, Isothermal amplification, CRISPR/Cas12a, Multiplexed detection, Aquatic monitoring, Point-of-care testing (POCT)

ACS Paragon Plus Environment
Published by ACS. This is the Author Accepted Manuscript issued with: Creative Commons Attribution License (CC:BY 4.0).
The final published version (version of record) is available online at DOI:10.1021/acssensors.6c00719. Please refer to any applicable publisher terms of use.

Graphical Abstract



Access to safe drinking water, sanitation, and proper hygiene (WASH) constitutes a critical public health priority and a key focus of international development policy.[1, 2] Microbial contamination in aquatic environments poses significant risks across rivers, lakes, reservoirs, groundwater, estuaries, and coastal waters,[3, 4] with waterborne illnesses estimated to cause over 2.2 million annual deaths worldwide and nearly $12 billion in economic losses.[5] According to World Health Organization (WHO) reports, only 71% of the global population has access to safely managed drinking water services.[6] This crisis highlights the urgent need for improved water quality management and sanitation infrastructure globally.

Waterborne diseases arise from the ingestion, inhalation, or contact with water contaminated by pathogenic microorganisms, with inadequate waste disposal, insufficient sanitation infrastructure.[7] Inefficient water treatment systems also serve as primary contributors to microbial contamination of drinking water that may lead to disease outbreaks.[8] In recent years, numerous studies have confirmed that pathogenic bacteria enter the environment primarily through wastewater from farms, slaughterhouses, and wastewater treatment plants (WWTPs), creating opportunities for wastewater-based epidemiology (WBE) to track pathogen sources.[9, 10] When integrated with clinical data, WBE can enhance pathogen surveillance by enabling timely detection of outbreak signals, thereby offering a powerful early warning tool for pathogen evaluation and disease surveillance.[11, 12]

Current pathogen detection methods for aquatic monitoring typically involve centralized laboratory analysis of water samples,[13] where culture-based methods require 1–2 days for results, failing to meet rapid detection demands.[14] Although nucleic acid amplification tests (NAATs), particularly gold standard polymerase chain reaction (PCR), offer specificity and sensitivity, they remain limited by time-consuming procedures, expensive instrumentation, specialized personnel, and laboratory dependence,[15] hindering their application in point-of-care testing (POCT).[16] Therefore, developing a POCT platform which meets the WHO's REASSURED criteria (real-time connectivity, ease of specimen collection and environmental friendliness, affordability, sensitivity, specificity, user friendliness, rapid and robust, equipment-free, and deliverable to end-users) not only facilitates early detection of community pathogens and clinical treatment, but also provides considerable public health value in reducing the global burden of diseases.

Clustered regularly interspaced short palindromic repeats and CRISPR-associated protein (CRISPR/Cas) systems employ single-guide RNA (crRNA) to achieve sequence-specific target binding with enhanced specificity, while the trans-cleavage activity of Cas enzymes further improves sensitivity.[17, 18] When coupled with isothermal amplification techniques such as recombinase-aided amplification (RAA),[19] recombinase polymerase amplification (RPA),[20] or loop-mediated isothermal amplification (LAMP),[21]

CRISPR/Cas12a systems have demonstrated improved sensitivity. However, direct one-pot detection remains challenging due to the potential inhibition of isothermal amplification by Cas enzymes. Although recent studies have employed optimized crRNA and primer designs to enhance efficiency, these approaches often face limitations in multiplexed detection.

In recent years, microfluidic technology has attracted widespread attention for POCT of pathogens due to their advantages in reagent consumption, analysis time, and operational complexity.[22] However, microfluidic systems often rely on bulky and expensive external accessories. Paper microfluidic biosensors, fabricated from cheap, flexible, and portable paper materials, enable the integration of automated sample preparation and detection on a single chip, while also offering user-friendly operation and compatibility with large-scale manufacturing.[23] Fluid flow is controlled through hydrophobic barriers and hydrophilic channels through capillary action without external power sources.[24] Although developed for pathogen detection, these biosensors have relied on cold-chain logistics and commercial instrumentation, imposing constraints on analytical throughput, which is a requirement that conventional paper microfluidic biosensors cannot fulfil.[25] This technological barrier has thus hindered the effective adaptation of aquatic pathogen detection onto integrated paper-based platforms.

In response to these challenges, we developed an integrated paper microfluidic platform for spatially multiplexed detection of pathogenic bacteria, engineered with a two-layer chip architecture that physically isolated isothermal amplification and CRISPR/Cas12a reaction chambers. This design facilitated the unidirectional transfer of amplification products to detection chambers through simple rotational alignment. All components were lyophilized to streamline analytical workflow and ensure reagent long-term stability. An engineered horseradish peroxidase (HRP) cascade-coupled crRNA modification system with DNA-conjugated labels was designed for colorimetric detection. Operation was enabled by environmentally friendly solar-powered and portable hardware for incubation and imaging, coupled with web application for quantitative analysis. This user-friendly and readily mass-producible platform thus overcomes the limitations of traditional paper microfluidic biosensors that require cold-chain logistics and commercial instrumentation. Sample-to-answer analysis was completed within 60 min, achieving a limit of detection (LOD) of 1 CFU/mL and a dynamic range of 1–10^7 CFU/mL, with high reproducibility (coefficient of variation, CV < 5%) and recovery rates exceeding 90%. Field validations in diverse aquatic environments (tap water, wastewater, and river water) confirmed the platform's robust performance, demonstrating strong consistency with gold standard PCR ($R^2 = 0.98$). Our aquatic monitoring platform

demonstrated significant POCT potential for public health protection and emerging epidemic monitoring, owing to its spatially multiplexed detection, field-ready design, and digital connectivity.

Experimental Section

PCR Assay and LAMP Assay

PCR assay and LAMP assay were performed on a Quant Studio 3 Real-Time PCR System. PCR reactions were performed in 20 μL, including 10 μL PCR Master Mix, 1.25 μL PCR primers (20 μM), 6.75 μL nuclease-free water, and 2 μL sample. PCR conditions consisted of initial denaturation at 95 °C for 3 min, followed by 40 cycles of denaturation at 95 °C for 15 s, annealing at 55 °C for 30 s, and extension at 72 °C for 30 s. LAMP primer sets for *Salmonella*, *Escherichia coli* (*E. coli*), *Clostridium perfringens* (*C. perfringens*), and *Brucella* are detailed in Table S1. LAMP reactions were performed in 20 μL, including 10 μL LAMP Master Mix, 3 μL LAMP primers (0.1 μM F3/B3, 0.8 μM FIP/BIP, and 0.6 μM LF/LB), 2 μL calcein (25 μM), 1 μL $MnCl_2$ (500 μM), 1 μL Gsp 2.0 DNA polymerase, 1 μL nuclease-free water, and 2 μL sample. Trehalose was added to reach a concentration of 10% (w/v) for lyophilization. The modified mixture was frozen at -20 °C for 4 h, and transferred to a Virtis lyophiliser operating at a vacuum pressure of 15.9 millitorr for 4 h. The lyophilized mixture was reconstituted and subjected to LAMP reactions as described.

RAA Amplification and CRISPR/Cas12a Detection

RAA primer sets for *Salmonella Typhimurium* (*S. Typhimurium*), *Bacillus cereus* (*B. cereus*), and *Vibrio parahaemolyticus* (*V. parahaemolyticus*) were designed using Primer-Basic Local Alignment Search Tool (BLAST) website and crRNA was designed on CRISPOR with sequences provided in Table S2. RAA system contained 12.5 μL rehydration buffer, 1 μL forward primer (10 μM), 1 μL reverse primer (10 μM), 1.3 μL magnesium acetate (MgAc), 1 μL sample, and nuclease-free water up to 25 μL with incubation at 39 ℃ for 20 min. CRISPR/Cas12a system contained reaction buffer, Cas12a (300 nM), crRNA (150 nM), ssDNA reporter (500 nM), RAA amplicons, and nuclease-free water up to 10 μL with incubation at 43 ℃ for 20 min. Different RAA temperatures (37, 39, 41, and 43 °C), concentration ratios of crRNA to Cas12a (0.1:1, 0.5:1, 1:1, and 5:1), ssDNA reporter concentrations (300, 400, 500, and 600 nM), and CRISPR/Cas12a temperatures (39, 43, 45, and 48 °C) were evaluated for improved sensitivity.

crRNA was designed based on target sequence and protospacer adjacent motif (PAM) site. To generate DNA templates for crRNA synthesis, two ssDNA were annealed at 95 °C for 5 min, followed by gradual

cooling to room temperature. The reaction mixture consisted of 2.5 μL forward primer (100 μM), 2.5 μL reverse primer (100 μM), and 45 μL nuclease-free water. crRNA synthesis was performed using a HiScribe T7 High-Yield RNA Synthesis Kit (NEB, UK). The reaction mixture consisted of 2 μL T7 reaction buffer, 2 μL T7 RNA polymerase mix, 2 μL NTP mix, 12 μL nuclease-free water, and 2 μL DNA template. Reverse transcription was performed at 37 °C for 3 h. 1 μL DNase I was added and incubated at 37 °C for 15 min to remove templates.

RPA Amplification and CRISPR/Cas12a Detection

RPA primer sets for *Staphylococcus aureus* (*S. aureus*), *Toxoplasma gondii* (*T. gondii*), and *Listeria monocytogenes* (*L. monocytogenes*) were designed using Primer-BLAST website and crRNA was designed on CRISPOR with sequences provided in Table S2. RPA pellet was rehydrated with a Master Mix containing 29.5 μL rehydration buffer, 2.1 μL forward primer (10 μM), 2.1 μL reverse primer (10 μM), 0.6 μL probe (10 μM), with sample and nuclease-free water up to 13.2 μL. Nucleic acid solution was added to each reaction mixture to yield concentrations of 420 nM for each primer and 120 nM for probe. 2.5 μL MgAc (280 mM) was then added to each tube followed by gentle mixing. The reaction mixture was centrifuged into the MgAc solution with incubation at 37 °C for 30 min.

CRISPR/Cas12a system contained 29.5 μL rehydration buffer, 3.7 μL nuclease-free water, 2.4 μL forward primer (10 μM), and 2.4 μL reverse primer (10 μM) added to an RPA TwistAmp basic enzyme pellet. 2.5 μL MgAc (280 mM) was added after dissolution. The reaction mixture was vortexed and briefly centrifuged to ensure homogeneity. 2 μL sample was added to 9 μL reaction mixture, with incubation at 37 °C for 30 min. For fluorescence detection, RPA-CRISPR/12a reaction was performed in 20 μL at 37 °C for signal generation, which consisted of NEB Buffer, Cas12a (0.1 μM), crRNA (0.12 μM), ssDNA reporter (0.1 μM), recombinant RNase inhibitor (10 U), DTT (2.5 mM), and 1 μL RPA amplicons.

Preparation of HRP-ssDNA-MB Probes and crRNA-HRP Coupled Amplification

A 50 μM HRP solution was prepared by dissolving 2 mg HRP in 1000 μL $NaHCO_3$ solution (0.1 M). A 1000-fold molar excess of azido-PEG4-NHS ester linker was added to this solution and the mixture was incubated at room temperature for 2 h. Excess linker was removed using a desalting column, followed by concentration of modified HRP through ultrafiltration. For DNA conjugation, 200 μL azido-modified HRP (10 μM) was reacted with 2 equivalents of 5'-DBCO-TEG-T25-biotin-3' DNA in phosphate buffered saline (PBS) buffer for 15 h, after which unreacted DNA was removed by ultrafiltration. Streptavidin-coated magnetic beads (40 μL) were washed with 600 μL PBS containing 0.1% Tween 20,

then incubated with 5 μL HRP-DNA-biotin conjugate (800 nM). The mixture was vortexed at 1,500 rpm for 5 min, followed by centrifugation at 20,000×g for 1 min to remove supernatant. The functionalized beads were washed at least 10 times with PBS-Tween to ensure complete removal of unbound HRP.

Following established protocols for crRNA coupling, crRNA mixture was prepared by combining 5 μL coupling mixture with a volume of NEB buffer. This solution was mixed with the functionalized magnetic beads and aliquoted into four tubes, each containing different nucleic acid concentrations in NEB buffer. Final reaction volume was adjusted to 60 μL and incubated at 37 °C for 40 min. After centrifugation, 30 μL supernatant was collected and mixed with 30 μL 3,3',5,5'-Tetramethylbenzidine (TMB) substrate. Fluorescence measurements were recorded at excitation/emission wavelengths of 570 nm. Colorimetric measurements were captured using a mobile phone camera and quantified using a custom web application.

Fabrication and Characterization of Paper Microfluidic Biosensor

Paper microfluidic biosensor was designed in CorelDraw and fabricated via wax-printing on Whatman Grade 1 Qualitative Filter Paper, followed by baking at 130 °C for 5 min (Figure 1a). The device architecture comprised a filter paper-based microfluidic chip integrated with a glass fiber disc (4 mm diameter) and sealed with a single-sided optical adhesive film on a plastic plate, featuring a compact 3 cm × 3 cm footprint per panel. The unfolded design incorporated sample preparation and detection zones. In Figure 1b, water samples were filtered through a 0.45 μm syringe filter, then lysed with buffer during 10-min room-temperature incubation. Nucleic acids were adsorbed onto the glass fiber, purified via 70% ethanol wash (25 μL), and eluted with nuclease-free water (30 μL) into hydrophilic microfluidic channels.

Reagent-preloaded devices were prepared by dispensing 20 μL LAMP reaction mixture into the chambers for isothermal amplification, while RAA-CRISPR and RPA-CRISPR systems received 12.5 μL isothermal amplification reaction mixture in first-layer wells followed by 12.5 μL CRISPR/Cas12a reaction mixture in corresponding second-layer wells, with all reagents lyophilized and sealed under transparent membranes for stability. For isothermal amplification-CRISPR detection, samples underwent 20-min incubation for amplification followed by 20-min CRISPR/Cas12a detection in adjacent wells after product transfer, with transparent membranes preventing evaporation and contamination. Results were visualized via mobile phone camera imaging and quantified using custom web application.

Operation Workflow of Paper Microfluidic Biosensor

The operational workflow of the paper microfluidic biosensor comprised sample preparation, reagent reconstitution, isothermal amplification, and rotational transfer for CRISPR/Cas12a detection (Figure 1a). Water samples were filtered through a 0.45 μm syringe filter to remove particulate matter, followed by lysis buffer incubation (10 min). Lysate was applied to the glass fiber disc embedded in the sample preparation zone of paper microfluidic device. After washing with 70% ethanol (25 μL) to remove inhibitors, nucleic acids were eluted with nuclease-free water (30 μL), flowing through wax-defined hydrophilic channels into the collection zone.

The device was unfolded to expose the dual-layer architecture. Upper chambers contained lyophilized isothermal amplification reagents (RAA/RPA), while lower chambers held lyophilized CRISPR/Cas12a complexes. After sealing with transparent adhesive films, the device was placed in a solar-powered incubator for isothermal amplification. The dual-layer design ensured physical isolation between amplification and detection zones. The upper layer was manually rotated clockwise after isothermal amplification, aligning amplification chambers above corresponding detection chambers. Finger pressure created capillary-driven flow, transferring amplicons into lower chambers. Following incubation for CRISPR/Cas12a detection, chambers were imaged under 365 nm LED excitation (fluorescence mode) or treated with HRP-substrate solution after magnetic separation, producing blue coloration quantified via web application (colorimetric mode).

Custom Hardware and Web Application

Solar-powered portable system consisted of an incubator featuring microprocessor-controlled temperature regulation (Tianyigf) with PT100 platinum resistance sensor (Chengda) and 40W PTC ceramic heaters (Chuangzhi) powered by a 12V DC supply, together with double-sided aluminum foil insulation for stable isothermal amplification. The system also included an ultraviolet (UV) detector incorporating a 365 nm LED array (Anteleisi) within a 3D-printed acrylic chamber with a light-absorbing interior, and an imaging detector combining a honeycomb light-diffusing assembly and soft-light panel for uniform illumination. Colorimetric quantification was performed using custom algorithms that executed color space transformation for spectral decomposition and normalized mean intensity calculation within user-defined regions of interest. The power system supported solar input (via photovoltaic controller), power banks, or lithium batteries, ensuring adaptability and sustainability.

Web application employed a decoupled client-server architecture, featuring a Vue.js-based frontend (HTML/CSS/JavaScript) for dynamic data visualization via ECharts, and a Python backend (FastAPI

framework) for computational processing, communicating through RESTful APIs with JSON payloads. Key functions included colour channel extraction and mean intensity calculation using OpenCV, concentration calibration via NumPy's polynomial regression, and image processing encompassing acquisition, grayscale conversion (weighted average method), and quantitative analysis through linear regression modeling. The system generated processed grayscale values and calculated concentrations, with all algorithms validated against standard reference materials to ensure analytical accuracy.

Water Sampling

Drinking water samples were collected from Class B private water supplies in Aberdeenshire (UK) at point-of-use kitchen taps to ensure relevance to human consumption. Wastewater samples were obtained from local WWTPs via Anglian Water Ltd (UK), using autosamplers programmed for 24-h composite sampling (50 mL aliquots every 30 min) to capture flow variations. Samples were immediately transferred to 1 L sterile containers and preserved in thermally insulated transport bags with ice packs. River water samples were collected from urban catchments in Edinburgh, Glasgow, Milton Keynes, and London, while commercial bottled water samples were acquired from local retailers to serve as reference controls.

Water samples underwent comprehensive physicochemical analysis using standardized protocols. A portable multi-parameter meter (Suijing, China) quantified pH, dissolved oxygen (DO; mg/L), total dissolved solids (TDS; mg/L), total nitrogen (TN), ammonium-N (NH_4^+-N; mg/L), and nitrate-N (NO_3^- N; mg/L). Additional parameters including oxidation-reduction potential (ORP; mV), electrical conductivity (EC; μS/cm), and water temperature (WT; °C), were measured using calibrated portable meters (Aipu, China). Triplicate measurements were performed at each sampling location to ensure data reproducibility, with strict adherence to quality control protocols throughout the analytical process.

Statistical Analysis

The means of triplicate experiments were calculated for repeatability analysis. All experiments were performed in triplicate, and at least three independent experiments were conducted unless otherwise stated. Standard deviation (SD) and relative standard deviation (RSD) were calculated using following equations.

$$Std = \sqrt{\frac{\sum (X-\alpha)^2}{n-1}} \qquad \text{Equation 1}$$

where *Std* is standard deviation, X is value of each replicate, α is mean of all replicates, and n is number of replicates.

$$RSD(\%) = \frac{Std}{\alpha} \times 100\% \qquad \text{Equation 2}$$

where *RSD* is relative standard deviation, *Std* is standard deviation, α is mean of all replicates.

Data were processed and visualized through Python 3 with Matplotlib library. Statistical analyses were performed using Python (SciPy and statsmodels libraries). The threshold for positive tests was established as 10% of the maximum fluorescence intensity. Signals from negative samples fell below the threshold, serving as a background noise baseline. The quantification of DNA copy numbers was achieved by extrapolation from a standard curve of known concentrations, plotted against the mean cycle threshold (C_t) values. LOD was calculated as 3σ/m, where σ is the SD of blank signal and m is the slope of calibration curve. Recovery rate was calculated based on the ratio of the recovered concentration to the known concentration using the following formula: $Recovery\ (\%) = C_{\text{recovered}} / C_{\text{known}} \times 100\%$.

One-way analysis of variance (ANOVA) determines whether statistically significant differences exist between the means of independent groups, with interpretation based on the calculated p-value. One-way ANOVA followed by Tukey's post hoc test was used for multiple comparisons between groups. When $p > 0.05$, observed inter-group mean differences are considered attributable to random variation rather than systematic effects. Conversely, $p < 0.05$ indicates that the probability of observed differences arising by chance alone is sufficiently low to conclude statistical significance between group means. Statistical significance was defined as $p < 0.05$.

Results

Principle of Paper Microfluidic Platform for Aquatic Monitoring

Water quality preservation represents one of the serious challenges of the 21st century. Inadequate sanitation compromised safe drinking water access for over one-third of the global population. Aligning with European Union (EU) Water Framework Directive's principle that water constitutes a vital heritage requiring protection,[26] a paper microfluidic platform combing spatially multiplexed isothermal amplification and CRISPR/Cas12a detection was developed for pathogen detection in aquatic environments (Figure 1). The device was designed using CorelDraw and fabricated through wax-printing, with reagents preloaded and lyophilized for POCT applications. Detection mechanisms relied on CRISPR/Cas12a-mediated cleavage of fluorophore/quencher-labeled ssDNA reporter (fluorescence detection) or HRP-conjugated ssDNA reporter (colorimetric analysis), enabling sensitive and specific dual-mode pathogen identification.

LbCas12a enzyme derived from *Lachnospiraceae* was employed for pathogen detection. Guided by crRNA, Cas12a binds to dsDNA targets. By programming crRNA module, Cas12a can be directed to any sequence downstream of PAM site. Upon target recognition, conformational changes in the Cas12a-crRNA-target complex activate trans-cleavage. To quantitatively assess Cas12a's nuclease activity, ssDNA reporters containing a 5' fluorophore and a 3' quencher were utilized, where fluorescence resonance energy transfer (FRET) resulted in signal quenching. In the presence of dsDNA targets, activated Cas12a cleaved reporters, separating fluorophore from quencher and restoring fluorescence. To enable multiplexed detection, the device incorporated spatially separated reaction chambers, each preloaded with target-specific reagents. For RAA/RPA-CRISPR assays, the upper layer chambers contained target-specific primer pairs, while the corresponding lower layer chambers were preloaded with Cas12a, target-specific crRNAs, and ssDNA reporters. The spatial separation of reaction reagents in dedicated chambers ensured that each reaction proceeded independently without cross-reactivity.

Isothermal amplification and CRISPR/Cas12a detection were physically separated into two distinct layers on a microfluidic chip to prevent interference. Nucleic acids extracted using paper origami device were subjected to isothermal amplification in the upper chambers. Subsequent rotation of layers aligned the upper and lower chambers, enabling directional transfer of amplicons to CRISPR/Cas12a detection chambers. Target-specific crRNAs guided Cas12a to recognize amplicons, triggering collateral cleavage of ssDNA reporters and generating fluorescent signals. For field testing, reaction reagents were preloaded and sealed with transparent membranes to prevent contamination. The entire assay was completed within 60 min, including paper-based nucleic acid extraction (15 min), isothermal amplification (20 min), CRISPR/Cas12a detection (20 min), and chip rotation (1 min). The operational simplicity was achieved through user-friendly design. Manual rotation served as a switch, converting the device from amplification mode (layers misaligned) to detection mode (layers aligned). This transfer mechanism prevented backflow contamination, enabled untrained operators to conduct tests, and reduced operation time.

Sample Processing and Isothermal Amplification Assay on Paper Microfluidic Biosensor

Enrichment strategies, nucleic acid extraction methods, and isothermal amplification approaches were evaluated to meet international standards requiring processing 100 mL water samples (Figure 2a; Figure S1). Based on cost-effectiveness and portability considerations, manual filtration using syringe filters was selected with paper-based nucleic acid extraction for sample processing. PCR results demonstrated that nucleic acids extracted via manual filtration achieved 80% of the yield obtained through ultrafiltration. As an efficient nucleic acid adsorption medium, glass fiber exhibits high binding capacity through

chaotropic salt-mediated interactions with silica-based surfaces. It provides exceptional biocompatibility, room-temperature stability, and compatibility with paper microfluidic biosensor. Whatman Grade GF/F glass microfiber filters were employed in this study, which were effective in retaining particles as small as 0.7 μm with an efficiency of 98%.

To evaluate elution efficiency, PCR assay was performed on nucleic acids retained by glass fiber as well as those obtained using a commercial nucleic acid extraction kit. The former method exhibited comparable performance, combining high binding efficiency (Recovery > 85%) and rapid processing (< 10 min), while maintaining purity (A260/A280 ratio of 1.8–2.0) suitable for downstream applications. However, a portion of unlysed bacteria entered the pores of glass fiber, hindering nucleic acid release. It was found that preheating elution buffer to 65 °C increased the recovery rate to 90%. This improvement may be attributed to the reduced buffer viscosity facilitating the dissociation of nucleic acids or the disruption of hydrogen bonds between nucleic acids and matrix to improve elution efficiency. Overall, the paper-based isothermal amplification assay demonstrated comparable performance to commercial kits with a shorter analysis time (60 min), thereby providing an efficient solution for aquatic monitoring.

Considering that LAMP reactions require 4–6 primers to target 6–8 regions,[27] LAMP primers were designed using PrimerExplorer and subjected to BLAST to evaluate their homology with other sequences. LAMP primers were designed based upon *Salmonella* InvA gene, *E. coli* malB gene, and *C. perfringens* cpa gene (Figure S2). Effective amplification occurred across different temperatures, with optimal performance at 63 °C. Consistent amplification was achieved across 5–30 μL, demonstrating volume-independent LAMP efficiency. Optimal performance was achieved in 20 μL with a calcein : Mn^{2+} ratio of 1:20 and FIP/BIP primer concentrations of 0.8 μM (*Salmonella*), 1.0 μM (*E. coli*), and 1.2 μM (*C. perfringens*). Calcien-based LAMP assay demonstrated a LOD of 20 copies per reaction (LOD: 1 copy/μL; Figure S3), a tenfold improvement over EvaGreen-based LAMP assay (LOD: 10 copies/μL; Figure S4, S5), which was comparable to PCR assay with a shorter analysis time (1 h VS 4 h; Figure S6).

It's noted that LAMP assay typically requires low-temperature (-20 °C) storage of enzyme components, presenting significant challenges for POCT in resource-limited settings.[28] To address this limitation, a lyophilization protocol was developed, where the optimized formulation incorporated 10% (w/v) trehalose as a lyoprotectant to preserve enzymatic activity. Stability assessment demonstrated that lyophilized reagents maintained consistent performance when stored at room temperature for up to 7 weeks, with no obvious variation in endpoint fluorescence (LOD: 1 copy/μL; ANOVA, $P > 0.05$; Figure S7). Validation study using bacteria-spiked tap water samples confirmed equivalent sensitivity between

lyophilized and liquid LAMP assays (LOD: 1 CFU/mL; ANOVA, $P > 0.05$; Figure S8). Therefore, lyophilization maintained satisfactory performance, not only eliminating cold-chain dependencies but also reducing processing steps and minimizing contamination risks.

Fluorescent Isothermal Amplification-CRISPR Detection

In the CRISPR/Cas12a system, excessive crRNA competitively sequestered Cas12a, leading to nonspecific cleavage of fluorescent reporters and delayed signal generation. Insufficient crRNA restricted the formation of functional ribonucleoprotein complexes and compromised sensitivity. Reaction conditions were thus optimized for RAA-CRISPR detection (Figure 3a). Peak fluorescence intensities were observed at a crRNA : Cas12a ratio of 0.5:1 for *B. cereus* and 1:1 for *S. Typhimurium*, while *V. parahaemolyticus* exhibited comparable signals across ratios (0.5:1–1:1). To balance cost-effectiveness and robustness, a 0.5:1 crRNA : Cas12a ratio and 500 nM ssDNA reporter were chosen. A compromise temperature suitable for most targets was determined, namely 39 °C for RAA assay and 43 °C for CRISPR/Cas12a detection. The optimized system demonstrated a dynamic range of 100–10^7 CFU/mL and a LOD of 100 CFU/mL, which outperformed most CRISPR-based biosensors in sensitivity and multiplexed capability (Figure 3b; Figure S9a; Table S3). Potential cross-reactivity was examined and fluorescent signals were observed exclusively in target bacteria (ANOVA, $P > 0.05$; Figure S10b). Three non-target bacteria, *Citrobacter freundii* (*C. freundii*), *Campylobacter jejuni* (*C. jejuni*), *Pseudomonas aeruginosa (P. aeruginosa*), exhibited no cross-reactivity and supported high specificity (Figure S10d).

To evaluate storage stability of RAA-CRISPR system, RAA and CRISPR/Cas12a reagents were lyophilized with 10% trehalose and stored at -20 °C, 4 °C, and room temperature for 4 weeks (Figure 3c). RAA fluorescence signal remained stable when stored at -20 °C, retaining 95.5% of initial intensity after 4 weeks. At 4 °C, the signal exhibited a slight decline to 90.6% over the same period. In contrast, storage at room temperature resulted in a gradual reduction in signal, beginning at week 2 and reaching 72.5% by week 4. The stability trends observed for RAA-CRISPR assay at room temperature closely mirrored those of RAA assay alone, with signal attenuation initiating at week 2 and stabilizing at 72.1% by week 4. After one week of storage, the signal of lyophilized reagents showed no significant deviation from that of liquid reagents ($p > 0.05$), with clear discrimination between negative and positive controls.

The ssDNA reporter concentration of RPA-CRISPR system was also optimized for detecting *S. aureus*, *T. gondii*, and *L. monocytogenes*. Figure 4a indicated that higher concentrations accelerated the reaction process into the plateau phase. Since equivalent fluorescence intensities were observed at 200, 400, and

800 nM (ANOVA, $P > 0.05$), 200 nM was selected to minimize costs. It was indicated that a 1:1 ratio of crRNA : Cas12a (50 nM) yielded maximum efficiency. The optimized system demonstrated a dynamic range of 5–10^5 CFU/mL, with a LOD of 5 CFU/mL comparable to PCR assay and outperforming RPA assay (LOD: 10 CFU/mL) (Figure 4b; Figure S9c). This improvement was attributed to the combination of RPA amplification and CRISPR/Cas12a's collateral cleavage activity. This performance represented at least a 2-fold improvement in sensitivity over reported CRISPR-based biosensors (Table S3).

The storage stability of RPA-CRISPR system was also evaluated (Figure 4c). RPA fluorescent signal demonstrated exceptional stability at -20 °C, retaining 96.3% of initial intensity after 4 weeks. Similarly, storage at 4 °C resulted in only a marginal signal reduction to 92.3%. In contrast, room temperature storage led to a gradual decline, with signal attenuation beginning at week 2 and reaching 82.6% by week 4. The RPA-CRISPR assay exhibited comparable stability trends at room temperature, with signal retention of 82.1% after 4 weeks, closely mirroring the performance of RPA assay alone. After one week under all conditions, the lyophilized reagents exhibited no significant signal deviation compared to their liquid counterparts ($p > 0.05$). These findings highlighted the advantage of lyophilization in preserving reagent performance while enhancing field applicability without cold chain dependency.

Spatially multiplexed Fluorescent Detection on Paper Microfluidic Biosensor

The spatially multiplexed detection capability of paper microfluidic biosensor was demonstrated by spiking tap water samples with different bacterial combinations. Only reaction chambers preloaded with LAMP primer sets targeting corresponding bacteria exhibited significant fluorescent signals (Figure S11). The paper-based LAMP system achieved a LOD of 1 CFU/mL for *Salmonella*, surpassing a microfluidic-based LAMP lateral flow assay (50 CFU) and a turbidity monitoring LAMP device (14 CFU).[29, 30] *E. coli* was also detectable at 1 CFU/mL, matching a LAMP-CRISPR lateral flow biosensor (1 CFU) and outperforming a propidium monoazide-modified LAMP assay (30 CFU).[28, 29] The LOD for *C. perfringens* (0.5 CFU) was lower than that of magnetic bead extraction-based LAMP assay (10 CFU) and a lateral flow biosensor targeting alpha toxin (1–10 CFU).[30, 31] These results highlighted the superior sensitivity and specificity of our biosensor for spatially multiplexed fluorescent detection.

To evaluate the performance of our biosensor, drinking water samples were collected from private supplies in Aberdeen, and wastewater samples were obtained from WWTPs. *E. coli* detection in drinking water was initially confirmed using the standard Quanti-Tray method. Our biosensor yielded consistent results, detecting *E. coli* in 5 samples but not in another 3 samples (Figure S12). However, *Salmonella*

was undetected in 8 drinking water samples. For wastewater analysis, our biosensor identified *E. coli* in 11 samples and *Salmonella* in 9 samples, aligning with PCR validation (Figure S13). This may be attributed to spatial and temporal heterogeneity reflecting local variations in bacterial concentrations in wastewater. Potential contributing factors include rainfall-induced dilution, which can reduce bacterial loads below detection limits. Such variability highlights the importance of repeated sampling to accurately monitor microbial contamination in wastewater (Figure S14; Figure S15).

The detection rate of *Salmonella* in drinking water was significantly lower than that of *E. coli*, probably because *E. coli* exhibited robust survival across broad temperature and pH ranges (6.5–8.5), while *Salmonella* demonstrated reduced viability in acidic conditions. This difference suggests that drinking water treatment processes may be less effective at eliminating *E. coli*. Detection rates and calculated concentrations of *Salmonella* and *E. coli* were significantly lower in drinking water than in wastewater. This disparity can be attributed to drinking water treatment processes that reduce the microbial load. In contrast, wastewater originates from diverse sources such as domestic wastewater and industrial discharge, which provide nutrient-rich environments conducive to bacterial growth and proliferation.

Spatially multiplexed Colorimetric Detection on Paper Microfluidic Biosensor

To further facilitate field testing of isothermal amplification technology, a dual-output detection platform combining fluorescence and colorimetric readouts was engineered, thereby maintaining analytical precision while enabling instrument-free interpretation. Fluorescent probes were replaced with HRP-ssDNA-magnetic bead probes to construct a colorimetric detection system that produced an enzyme-mediated color change in response to target presence. A time-dependent color reference scale based on standardized responses was established, enabling semiquantitative analysis by visual comparison. In Figure 5a, when target gene was present, crRNA guided Cas12a to recognize and cleave target fragment in a cis-acting manner. Trans-cleavage activity of the complex was activated, enabling efficient cleavage of ssDNA reporters, thereby facilitating signal transmission. The enzyme-modified probes were finally introduced into the reaction mixture, enabling cascade amplification and visual detection.

Due to its high stability and amplification capability, HRP was selected as the reporter enzyme, conjugated to MBs via ssDNA reporters. Activated Cas12a-crRNA complexes effectively cleaved ssDNA-linked HRP-MB conjugates. Under magnetic separation, MBs were immobilized at the bottom of the container, while released HRP remained in the supernatant. Transferring the supernatant to a TMB solution resulted in a catalytic reaction that produced blue color. In the absence of target gene, Cas12a-crRNA complex

remained inactive and prevented HRP-MB separation. HRP remained bound to MBs under magnetic force, leaving no free HRP in the supernatant to catalyze TMB, so no color change occurred.

As presented in Figure 5b, this cascaded amplification strategy amplified ssDNA cleavage rate differences across concentration gradients (10–10^7 CFU/mL, R^2 = 0.98), yielding a LOD of 10 CFU/mL. TMB substrate exhibited concentration-dependent color progression from light to dark blue, with extracted colorimetric signals maintaining excellent linearity (R^2 = 0.95). The paper-based colorimetric isothermal amplification-CRISPR system achieved rapid detection ($\leqslant$ 30 min), which may be attributed to the enhanced sensitivity caused by HRP conjugation. This strategy established a new solution for POCT diagnosis through quantitative performance with linear signal and compatibility with colorimetric readout.

To evaluate storage stability of colorimetric detection, reagents were lyophilized with 10% trehalose and stored at -20 °C, 4 °C, and room temperature for 4 weeks (Figure 5c). LAMP colorimetric signal exhibited high stability at -20 °C, retaining 95.8% of initial intensity after four weeks, while storage at 4 °C resulted in a slight decrease to 91.9%. In contrast, room temperature storage led to a gradual decline, with signal attenuation initiating at week 2 and reaching 83.7% by week 4. RAA-CRISPR colorimetric signal retained 93.6% (-20 °C), 88.4% (4 °C), and 68.5% (RT), while RPA-CRISPR colorimetric signal retained 93.7% (-20 °C), 88.6% (4 °C), and 78.5% (RT) under identical conditions. It's noted that all lyophilized reagents maintained acceptable signal deviations after 4 weeks across storage conditions, highlighting the lyophilized paper-based colorimetric isothermal amplification-CRISPR strategy for POCT diagnosis.

High-Throughput Paper Microfluidic Biosensor for Aquatic Pathogen Detection

To meet the urgent need for pathogen detection in water quality monitoring, our platform integrated solar-powered portable incubation/imaging hardware, paper microfluidic biosensor, and mobile phone with custom web application (Figure S16). The incubator maintained a stable temperature during amplification process, with fluctuations within ± 0.5 °C. Figure 6a illustrated the workflow for storing lyophilized reagents in microchannels, which supported isothermal amplification-CRISPR detection. Mobile phone-captured images were processed through an analytical pipeline that constructed a calibration curve from standard concentrations (grayscale linear regression, $R^2 > 0.98$) for bacterial quantification. The image analysis web application featured a frontend interface (Vue.js framework with ECharts visualization) for user interaction, and a Python FastAPI backend employing RESTful APIs for data processing. The platform is thus not only cost-effective, user-friendly, and readily mass-producible, but it also shows significant potential for translating our pathogen detection strategy into POCT applications.

On the other hand, a hierarchical paper microfluidic biosensor was developed to achieve 96-plex parallel detection to address throughput limitation (12-fold enhancement; Figure S17). Through a radially symmetric fluidic network, capillary-driven flow from a central inlet distributed reagents to main channels, each of which bifurcated into X-shaped sub-channels across the multilayer substrate. This ensured uniform reagent delivery while maintaining strict separation of all reaction chambers. This design demonstrated exceptional sensitivity (LOD: 10 CFU/mL), reproducibility (coefficient of variation (CV) < 5%), and accuracy (recovery rate > 90%). By combining high-throughput capacity (96 samples/device) and robust performance, this design established a new paradigm for large-scale aquatic monitoring with laboratory-grade sensitivity and POCT practicality.

According to WHO guidelines, fecal indicator bacteria (FIB), such as *E. coli*, are widely recognized as essential microbial indicators for evaluating fecal contamination in aquatic monitoring. For paper-based colorimetric LAMP biosensor, *E. coli* was undetected in Sample 5 but present in other wastewater samples at concentrations ranging from 4.23×10^7 to 7.89×10^8 CFU/L. *C. perfringens* was not detected in any samples, aligning with fluorescent LAMP assay results (Figure 6b; Figure S18). One plausible explanation is that the primary contamination source was domestic wastewater containing abundant human fecal matter, which typically harbored *E. coli* as a dominant gut microbiota. In contrast, *C. perfringens* was more strongly associated with livestock farming wastewater. These findings suggested that elevated bacterial contamination, rather than helminth infections, posed a significant public health risk.

Salmonella was undetected in Samples 4–6 but present in other samples at concentrations of 5.21×10^6 to 4.75×10^7 CFU/L, consistent with levels reported in Roma wastewater. Similarly, high *Salmonella* concentrations were documented in municipal wastewater in Europa, whereas a Venice study found only mild contamination (33% of samples).[32] The presence of *Salmonella* in wastewater may reflect local epidemiological trends. For instance, *Salmonella*-contaminated SFC chicken products in MK supermarkets were recently recalled, as reported by the Daily Mail. This suggested that *Salmonella* may enter the human food chain and be excreted into wastewater, though further epidemiological tracing is needed to confirm this pathway.

Similarly, wastewater from aquaculture ponds and farmland in Vietnam exhibited severe contamination with total coliforms (1.3×10^8 CFU/L), *E. coli* (1.1×10^7 CFU/L), and *Salmonella* (10^9 MPN/L), though helminth egg concentrations remained below WHO thresholds (< 1 egg/L).[33] Complementary studies in Italian WWTPs detected total coliforms, enterococci, *E. coli*, and *C. perfringens*, highlighting the need to evaluate wastewater treatment efficacy and reuse risks, particularly in light of new EU legislations on

minimum water reuse standards.[34] Current WHO guidelines for safe reuse have established thresholds (*E. coli*: $\leqslant$ 10^3 CFU/100 mL; *Salmonella*: 10 CFU/100 mL; *Cryptosporidium*: $\leqslant$ 1 oocyst/L), emphasizing the urgency of enhancing wastewater treatment to meet public health objectives.

Paper-based colorimetric RAA-CRISPR biosensor revealed distinct pathogen distribution patterns, with *S. Typhimurium* undetected in samples 4–6 but present at 3.24×10^5–4.59×10^6 CFU/L in other samples, where seasonal rainfall amplified fecal runoff from anthropogenic and agricultural sources. *B. cereus* exhibited detection ranges of 1.28×10^5–7.16×10^5 CFU/L (absent in samples 4–5), with its chlorine-resistant spores enabling post-treatment persistence (10–10^3 CFU/L) in dairy and food-processing effluents. It's noted that *V. parahaemolyticus* was undetectable across all samples, consistent with its halophilic ecology and limited inland prevalence,[35] though its documented seasonal blooms in coastal waters highlighted persistent recreational exposure risks. These findings demonstrated how pathogen characteristics and anthropogenic factors influenced wastewater contamination.

Paper-based colorimetric RPA-CRISPR biosensor identified variable *S. aureus* contamination (5.47×10^5–5.65×10^6 CFU/L) across samples, with complete absence in samples 4–5, consistent with levels reported in Spanish WWTPs (6.8×10^5 CFU/L).[36] Genomic analysis revealed multiple staphylococcal clonal complexes, including both hospital-associated (CC5) and community-associated (CC8) strains, suggesting diverse anthropogenic sources. However, *T. gondii* was undetectable in our samples despite reported contamination in Qinghai Province, China (30–2300 oocysts; 2.2% positivity),[37]) likely reflecting regional differences in livestock reservoirs (sheep/yaks) and slaughterhouse practices. Similarly, *L. monocytogenes* showed sample-specific distribution (3.24×10^5–8.75×10^5 CFU/L) with complete recovery (> 90%) compared to PCR validation (Table S4).

On the other hand, extensive epidemiological evidence confirms that natural water bodies function as critical reservoirs and transmission vectors for pathogenic bacteria. River systems exhibit particularly pronounced fecal contamination due to sustained anthropogenic inputs. Pathogens in sediments are periodically resuspended into water bodies, forming dynamic exposure pathways, further exacerbating health risks for downstream communities. To bridge the gap between laboratory-based diagnostics and real-world monitoring, our platform was transported to the 16 river sites spanning four urban centers (Edinburgh, Glasgow, Milton Keynes, and London; Figure 6b), with replicate sampling at each location to ensure robust spatial representation of microbial contamination.

Paper-based colorimetric LAMP biosensor revealed *E. coli* contamination (4.29×10^4–7.19×10^6 CFU/L) across all samples, contrasting with sporadic *C. perfringens* detection. There was a divergence from reported concentrations in South Africa's Apies River (1.72×10^5–6.02×10^5 CFU/L) and Peruvian detection rates (50%).[38] This disparity reflected that facultative anaerobic *E. coli* dominated warm-blooded gut microbiomes and persisted in aerobic waters, whereas obligate anaerobic *C. perfringens* rapidly inactivated. Spatial analysis identified peak *E. coli* loads at high-density urban sites (Sites 14–16) with compromised sanitation, while secondary elevation at Site 5 (2.33×10^3–5.94×10^4 CFU/L) implicated medical effluent containing bioactive residues. Pristine watersheds (Sites 7/10) showed minimal contamination, whereas *Salmonella* exhibited livestock-dependent gradients ($p < 0.01$), with absence in undisturbed sites but concentrations mirroring global agricultural watershed data.[39] These findings linked anthropogenic pressures to pathogen loads, demonstrating how land use and microbial physiology jointly influence pollution regimes in aquatic systems.

Paper-based colorimetric RAA-CRISPR biosensor revealed distinct pathogen distribution patterns, with *S. Typhimurium* absent in Sites 2/7/10 and *B. cereus* undetected in Sites 2/7/8/10. *V. parahaemolyticus* was uniquely identified in coastal Site 3 (4.85×10^4 CFU/L) and harbor Site 4 (6.61×10^5 CFU/L), concentrations markedly exceeding typical estuarine levels (10–10^4 CFU/L at 2–20‰ salinity). This marine-freshwater dichotomy reflected the halophilic ecology of *V. parahaemolyticus*, whose survival in freshwater depends on seawater intrusion events. Reduced recovery rates (91.49% and 90.12% at Sites 3 and 4, respectively) indicated significant matrix interference from marine components. Ion competition ($Na^+/Cl^-/Mg^{2+}/Ca^{2+}$) may alter the cellulose surface charge and allow particulate organic matter to occupy binding sites. These findings highlighted the necessity for seawater-specific pretreatment protocols (desalination, chelation, or selective filtration) to address osmotic and particulate interferences.

Paper-based colorimetric RPA-CRISPR biosensor consistently detected *L. monocytogenes* across all samples (4.76×10^4–6.92×10^6 CFU/L), with concentrations comparable to Eastern Cape Province, South Africa (2.0×10^4–3.6×10^6 CFU/L).[40] One-way ANOVA confirmed significant concentration variations by water type ($p < 0.05$), demonstrating elevated loads in WWTP effluents and urban surface waters. This aligned with global culture-based prevalence data showing marked geographical variation. Detection rates were higher in South African rivers (50%) and Californian watersheds (43%), while detection rates were lower in Swiss (12.8%) and Canadian (10%) waters, and remained undetected in pristine environments in Austria and Wales.[41] *L. monocytogenes* was prevalent in areas impacted by human activities and absent

from undisturbed ecosystems, providing compelling evidence that human activities transform watersheds into persistent environmental reservoirs.[42]

S. aureus was undetected in Sites 2/7 but present elsewhere (3.34×10^4–6.64×10^5 CFU/L), while *T. gondii* exhibited unexpectedly high recoveries (104.76–103.35%) in Sites 14–15 despite being undetectable in wastewater controls. This discrepancy likely reflects multiple factors. The obligatory intracellular life cycle of *T. gondii* may result in extreme environmental dilution (< 1 oocyst/L) due to feline host and UV degradation. Wastewater matrix effects such as organic interferents may inhibit nucleic acid amplification, and recovery calculations using laboratory-modified tachyzoites (lacking oocyst walls) may overestimate on-site efficiency. These findings aligned with global patterns of precipitation-mediated pathogen transport, evidenced by São Paulo's rainy-season detection rates (7.7%) and California's seasonal mussel contamination peaks,[43] demonstrating hydrology's pivotal role in mobilizing waterborne pathogens across aquatic systems. The inflation of recoveries highlighted the need for environmental oocyst standards, particularly given the risk of cross-reactivity with *Cryptosporidium*/*Giardia* and particulate interference in low-background samples.

Discussion

Global water challenges encompass household/commercial water provision and wastewater management. Microbial pathogens, introduced into rivers and drinking water systems via fecal contamination from infected humans, livestock, wildlife, and untreated wastewater, pose significant public health risks. Aquatic monitoring plays a critical role in clarifying transmission pathways, identifying outbreak risk factors, and understanding pathogen dissemination within populations.[44] Although molecular techniques have improved the precision of pathogen detection tools, routine implementation of pathogen monitoring in resource-limited settings remains constrained by logistical and technical challenges.

Although CRISPR technology has improved the specificity of isothermal amplification, most biosensors depend on commercial nucleic acid extraction kits, refrigerated liquid reagents, and laboratory instrumentation. Our paper microfluidic platform combined isothermal amplification-CRISPR with enrichment, extraction, amplification, detection, and analysis to enable spatially multiplexed detection. A dual-layer chip architecture with physically isolated chambers was employed for isothermal amplification and CRISPR/Cas12a detection. Rotation allowed for unidirectional transfer of amplicons, eliminating the risk of cross-contamination. To minimize non-specific amplification, primers were designed with high specificity using bioinformatic screening against non-target genomes. Reaction temperatures were

optimized to balance amplification efficiency and specificity. The dual-layer architecture separated amplification and detection chambers, preventing false positives. CRISPR/Cas12a served as a secondary specificity detection method, recognizing only authentic amplicons through PAM sequence and crRNA complementarity verification. All reagents were lyophilized to ensure operational simplicity and long-term stability. Environmentally friendly solar-powered incubation/detection devices were fabricated, which delivered results through visual interpretation or web application-based quantitative analysis. Different isothermal amplification strategies were incorporated to demonstrate the versatility and compatibility of our platform across diverse nucleic acid detection methods (Table S5).

To further facilitate field testing of isothermal amplification technology, a DNA-labeled HRP-cascaded crRNA-modified system was developed for colorimetric detection, with LODs of 10 CFU/mL, Dynamic range: 10–10^7 CFU/mL, high reproducibility (CV < 5%), low batch-to-batch variation (< 6%), and recovery rates exceeding 90%. The entire assay was completed within 60 min, including paper-based nucleic acid extraction (15 min), isothermal amplification (20 min), CRISPR/Cas12a detection (20 min), and chip rotation (1 min). The use of low-cost materials, simplified reagent compositions, and minimal instrumentation reduced overall costs by 70–80% compared to standard laboratory methods, with an estimated cost of approximately £2.5 per test. Future large-scale manufacturing of paper microfluidic devices could further reduce the cost for routine environmental surveillance. This platform enabled near real-time detection of pathogens by wirelessly transmitting data, including pathogen type and quantitative concentration (derived from colorimetric intensity during trans-cleavage, with linear $R^2 > 0.98$). The modular device architecture also supports scalable integration of additional pathogens and compatibility with large-scale production. Successful field validation in diverse aquatic environments (tap water, wastewater, and river water) demonstrated strong consistency with gold standard PCR ($R^2 = 0.98$), further validating its feasibility in meeting the high-throughput detection needs of aquatic monitoring and its potential for scalable deployment in environmental surveillance applications.

Environmental water samples, particularly from river systems, represent a complex biological matrix with numerous inhibitors. Humic acids can inactivate DNA polymerases by binding to enzymes or interfere with nucleic acid hybridization. Divalent metal ions may denature proteins, while polysaccharides and proteins hinder molecular diffusion. To overcome these challenges and address wastewater matrix complexity, syringe filtration (0.45 μm) was employed to remove particulate matter and associated inhibitors including solids and algae. Nucleic acids were selectively captured on glass fiber disks functionalized with silica-based chemistry, which preferably bound nucleic acids under chaotropic

conditions while suppressing co-adsorption of humic substances and polysaccharides. Sequential washing steps with ethanol buffers further removed residual inhibitors without compromising nucleic acid retention. Wax-defined hydrophobic channels and sealing structures limited the reaction mixture's exposure to the environment and prevented contamination. PCR validation confirmed that extracted DNA was amenable to amplification, demonstrating robust resistance to inhibitor interference. The isothermal amplification system also exhibited tolerance to common environmental inhibitors through the use of Bst polymerase. Internal controls were included to monitor potential inhibition in individual samples.

Our platform demonstrated some advantages for POCT detection, including integration of sample-to-answer workflow without centralized laboratories, lyophilized reagents enhancing stability and user-friendliness, solar-powered operation enabling field testing, and spatially multiplexed detection capability addressing diverse pathogens. Compared to microfluidic platforms requiring pneumatic pumps, our rotation-based transfer mechanism reduced instrumentation dependency while maintaining reproducibility (CV < 5%). It's noted that our platform reduced the cost of bacterial detection by 70–80% compared to laboratory-based methods. The dynamic range covered environmentally relevant concentrations for bacteria (10–10^7 CFU/mL) and LODs of 10 CFU/mL. Comparison with other CRISPR-based biosensors (Table S3) revealed that our platform achieved comparable or superior performance. For instance, an RPA/LAMP assay achieved a LOD of 50 CFU/mL for E. coli detection in 60 min[45], while an RAA-CRISPR assay detected V. parahaemolyticus with a LOD of 100 CFU/mL in 60 min[46]. Furthermore, an RPA-CRISPR assay reported a LOD of 8 CFU/mL for S. aureus detection in 70 min[47]. Therefore, our platform represents an advancement toward POCT application, balancing analytical performance with operational feasibility for aquatic pathogen surveillance.

However, studies on the storage stability of lyophilized reagents indicated efficient storage at room temperature for one month, but long-term stability beyond 3 months under field storage conditions requires further validation. Reconstitution consistency may vary among operators, potentially affecting reproducibility and necessitating standardized protocols. Quantitative accuracy depends on colorimetric intensity measurements, though our web application incorporates calibration algorithms to compensate for these variations. Sensitivity can also be compromised in samples with extremely low bacterial loads. Correlating microbial abundance with clinical infection rates for quantitative risk assessment remains challenging, as it is influenced by dynamic environmental variables. Future investigation will focus on optimizing capture-wash-elute purification, such as using cationic polymer-modified cellulose.

The persistence and proliferation of bacteria in surface waters are governed by complex interactions among climatic and physicochemical factors. Temperature emerged as a primary determinant, with the measured range (19.1–22.4 °C) in this study, consistent with established thermal optimum for *Salmonella* and *E. coli* (summer proliferators) versus rotavirus and norovirus (winter-persistent). Nutrient availability modulated microbial ecology, particularly in rivers receiving treated wastewater or agricultural runoff. Our results revealed substantial nitrogen inputs (TN: 1.51–2.27 mg/L; NH_4^+-N: 0.52–1.53 mg/L; NO_3^--N: 0.12–0.24 mg/L) characteristic of watersheds with intensive fertilizer use, while dissolved oxygen levels (5.66–6.56 mg/L) reflected balanced aerobic conditions. This highlighted the need for multidimensional aquatic monitoring, particularly in catchments impacted by human activities.

On the other hand, municipal wastewater containing microbial communities is continuously discharged into aquatic systems, promoting the proliferation of pathogenic microorganisms.[48] These contaminants re-enter human populations through drinking water contamination, agricultural irrigation, or recreational water exposure. WBE has emerged as a transformative public health tool, analyzing wastewater biomarkers to monitor public health.[49] During the COVID-19 pandemic, WBE proved valuable for infectious disease surveillance, overcoming limitations of clinical systems that underestimated disease incidence due to undiagnosed cases and reporting failures.[50] Our paper microfluidic platform further demonstrated that wastewater monitoring could provide early detection of emerging pathogens at the community level through primer and reporter gene design modifications.

Despite substantial progress in freshwater quality management through EU legislation, including the Water Framework Directive, most European water bodies continue to fall short of achieving good ecological status.[51] Although current EU policies target pollution reduction and over-abstraction to safeguard water quality for both human and ecological needs, European Environment Agency's latest assessment confirmed persistent failures to meet minimum thresholds across lakes, rivers, estuaries, and coastal waters.[52] Our UK urban river monitoring data substantiated these findings, revealing widespread surface water contamination in urban and peri-urban areas that posed public health risks. Therefore, our platform established a promising solution for the next generation of aquatic sentinel monitoring systems capable of tracking temporal and spatial trends and emerging health hazards.

Conclusion

In summary, we developed a paper microfluidic platform for aquatic pathogen detection that integrated low-cost paper microfluidic biosensors with environmentally friendly solar-powered portable

incubation/imaging hardware and web application for quantitative analysis. The platform combined efficient bacterial extraction with isothermal amplification and CRISPR/Cas12a detection, enabling rapid sample-to-result testing within 60 min. Exceptional analytical performance was demonstrated, achieving a LOD of 1 CFU/mL, a dynamic range of 1–10^7 CFU/mL, high reproducibility (CV < 5%), and recovery rates exceeding 90%. Field validation in diverse aquatic environments confirmed the platform's feasibility, demonstrating 98% consistency with gold standard PCR. This platform presented a powerful solution for aquatic monitoring in resource-limited settings, with significant implications for protecting public health and monitoring emerging epidemics.

Supporting Information

The Supporting Information is available free of charge.

Additional materials and reagents; target DNA template synthesis; PCR assay and LAMP assay; analytical workflow of paper microfluidic platform; Optimization of calcein-based LAMP assay parameters; Analytical sensitivity of calcein-based LAMP assay and EvaGreen-based LAMP assay, PCR assay; Analytical specificity of calcein-based LAMP assay; Long-term stability assessment of lyophilized LAMP reagents; Performance evaluation of paper microfluidic biosensors in spiked samples; Analytical sensitivity of PCR, RAA, and RPA assays; Analytical specificity of LAMP, RAA, and RPA assays; LAMP assay on paper microfluidic biosensor for spatially multiplexed detection or detection in aquatic matrices; PCR assay for *Salmonella* and *E. coli* detection in aquatic matrices; Performance evaluation of PCR assay in aquatic matrices; Solar-powered custom hardware and web application; Design of small-scale and high-throughput paper microfluidic chips; On-site LAMP assay on paper microfluidic biosensor in aquatic matrices; Sequences of LAMP primers for bacterial detection; Sequences of RAA primers, RPA primers, crRNA, and ssDNA reporters; Comparison with other CRISPR-based biosensors; Validation of PCR assay for bacterial detection in aquatic matrices (DOC). Video S1. Demonstration of the operation workflow of the paper microfluidic biosensor (MP4).

Terms & Conditions

Most electronic Supporting Information files are available without a subscription to ACS Web Editions. Such files may be downloaded by article for research use (if there is a public use license linked to the relevant article, that license may permit other uses). Permission may be obtained from ACS for other uses through requests via the RightsLink permission system: http://pubs.acs.org/page/copyright/permissions.html.

Author Information

Corresponding Author

Zhugen Yang - *Faculty of Engineering and Applied Sciences, Cranfield University, Cranfield, MK43 0AL, UK,*

Email: zhugen.yang@cranfield.ac.uk

Author

Yuwei Pan - *Faculty of Engineering and Applied Sciences, Cranfield University, Cranfield, MK43 0AL, UK; College of Chemical and Biological Engineering, Zhejiang University, Hangzhou, 310058, China*

Author Contributions

Y. P.: Experiments, data analysis, figure drawing, and writing–original draft. Z. Y.: Conceptualization, project administration, investigation, review & editing, and supervision.

Notes

The authors declare no competing financial interest.

Acknowledgments

The work was supported by UKRI NERC Fellowship grant (NE/R013349/2), UK RAE (FF\1920\1\36), UKRI NERC N-WESP (NE/V010441/1), UK Health Security's Environmental Monitoring for Health Protection and Anglian Water. ZY thanks Leverhulme Trust Research Leadership Awards (RL-2022-041). The authors acknowledge Scottish Water, Anglian Water, as well as water supplies from Aberdeenshire for provision of samples.

References

1. Wolf, J.; Hubbard, S.; Brauer, M.; Ambelu, A.; Arnold, B. F.; Bain, R.; Bauza, V.; Brown, J.; Caruso, B. A.; Clasen, T.; Colford, J. M.; Jr, Freeman, M. C.; Gordon, B.; Johnston, R. B.; Mertens, A.; Prüss-Ustün, A.; Ross, I.; Stanaway, J.; Zhao, J. T.; Cumming, O.; Boisson, S. Effectiveness of interventions to improve drinking water, sanitation, and handwashing with soap on risk of diarrhoeal

disease in children in low-income and middle-income settings: a systematic review and meta-analysis. *Lancet* **2022**, *400* (10345), 48–59, DOI: 10.1016/S0140-6736(22)00937-0

2. Ray, I.; Smith, K. R. Towards safe drinking water and clean cooking for all. *Lancet Glob. Health* **2021**, *9* (3), e361–e365, DOI: 10.1016/S2214-109X(20)30476-9

3. Seymour, J. R.; McLellan, S. L. Climate change will amplify the impacts of harmful microorganisms in aquatic ecosystems. *Nat. Microbiol.* **2025**, *10* (3), 615–626, DOI: 10.1038/s41564-025-01948-2

4. Farkas, K.; Walker, D. I.; Adriaenssens, E. M.; McDonald, J. E.; Hillary, L. S.; Malham, S. K.; Jones, D. L. Viral indicators for tracking domestic wastewater contamination in the aquatic environment. *Water Res.* **2020**, *181*, 115926, DOI: 10.1016/j.watres.2020.115926

5. Kunz, J. M.; Lawinger, H.; Miko, S.; Gerdes, M.; Thuneibat, M.; Hannapel, E.; Roberts, V. A. Surveillance of waterborne disease outbreaks associated with drinking water—United States, 2015–2020. *MMWR Surveill. Summ.* **2024**, *73* (1), 1–23, DOI: 10.15585/mmwr.ss7301a1

6. Hope, R. Four billion people lack safe water. *Science* **2024**, *385* (6710), 708–709, DOI: 10.1126/science.adr3271

7. Khodaparast, M.; Sharley, D.; Marshall, S.; Beddoe, T. Advances in point-of-care and molecular techniques to detect waterborne pathogens. *npj Clean Water* **2024**, *7*, 74, DOI: 10.1038/s41545-024-00368-9

8. Singh, S.; Sivaram, N.; Nath, B.; Khan, N. A.; Singh, J.; Ramamurthy, P. C. Metal organic frameworks for wastewater treatment, renewable energy and circular economy contributions. *npj Clean Water*, **2024**, *7*, 124, DOI: 10.1038/s41545-024-00408-4

9. Ghosh, S.; Smadi, M.; Bivins, A. In Situ performance of granular activated carbon for sampling viruses and bacteria from wastewater: Toward quantitative passive sampling for wastewater-based epidemiology. *Water Res.* **2025**, *288* (A), 124605, DOI: 10.1016/j.watres.2025.124605

10. Aßmann, E.; Greiner, T.; Richard, H.; Wade, M.; Agrawal, S.; Amman, F.; Böttcher, S.; Lackner, S.; Landthaler, M.; Mangul, S.; Munteanu, V.; Psomopoulos, F.; Smith, M.; Trofimova, M.; Ullrich, A.; von Kleist, M.; Wyler, E.; Hölzer, M.; Irrgang, C. Augmentation of wastewater-based epidemiology with machine learning to support global health surveillance. *Nat. Water* **2025**, *3*, 753–763, DOI: 10.1038/s44221-025-00444-5

11. Nnachi, R. C.; Sui, N.; Ke, B.; Luo, Z.; Bhalla, N.; He, D.; Yang, Z. Biosensors for rapid detection of bacterial pathogens in water, food and environment. *Environ. Int.* **2022**, *166*, 107357, DOI: 10.1016/j.envint.2022.107357

12. Grassly, N. C.; Shaw, A. G.; Owusu, M. Global wastewater surveillance for pathogens with pandemic potential: opportunities and challenges. *Lancet Microbe* **2025**, *6* (1), 100939, DOI: 10.1016/j.lanmic.2024.07.002

13. Hill, R.; Stentiford, G. D.; Walker, D. I.; Baker-Austin, C.; Ward, G.; Maskrey, B. H.; van Aerle, R.; Verner-Jeffreys, D.; Peeler, E.; Bass, D. Realising a global One Health disease surveillance approach: insights from wastewater and beyond. *Nat Commun.* **2024**, *15* (1), 5324, DOI: 10.1038/s41467-024-49417-4

14. Gigante, V.; Murtagh, M.; Bachmann, T. T.; Rocke, T.; Trainor, B. W.; Poutanen, S. M.; Roberts, T.; Vila, J.; Cameron, A. Diagnostics for priority bacterial pathogens: global gaps and research needs for curbing antimicrobial resistance in low-resource settings. *Lancet Microbe.* **2026**, 101385, DOI: 10.1016/j.lanmic.2026.101385

15. Adedokun, G.; Alipanah, M.; Fan, Z. H. Sample preparation and detection methods in point-of-care devices towards future at-home testing. *Lab Chip* **2024**, *24* (15), 3626–3650, DOI: 10.1039/d3lc00943b

16. Land, K. J.; Boeras, D. I.; Chen, X. S.; Ramsay, A. R.; Peeling, R. W. REASSURED diagnostics to inform disease control strategies, strengthen health systems and improve patient outcomes. *Nat. Microbiol.* **2019**, *4* (1), 46–54, DOI: 10.1038/s41564-018-0295-3

17. Li, L. J.; Zhang, D. Q.; Zhang, Z. Y.; Zhang, B. H. CRISPR/Cas: a powerful tool for designing and improving oil crops. *Trends Biotechnol.* **2025**, *43* (4), 773–789, DOI: 10.1016/j.tibtech.2024.09.007

18. Zheng, Y. J.; Sun, X. Y.; Li, X. J.; Lei, J.; Son, E. Q. CRISPR/Cas system-based strategies for pathogenic bacteria detection. *Trends Anal. Chem.* **2025**, *194* (A), 118497, DOI: 10.1016/j.trac.2025.118497

19. Li, X.; Zhu, S.; Zhang, X.; Ren, Y.; He, J.; Zhou, J.; Yin, L.; Wang, G.; Zhong, T.; Wang, L.; Xiao, Y.; Zhu, C.; Yin, C.; Yu, X. Advances in the application of recombinase-aided amplification combined with CRISPR-Cas technology in quick detection of pathogenic microbes. *Front. Bioeng. Biotechnol.* **2023**, *11*, 1215466, DOI: 10.3389/fbioe.2023.1215466

20. Monteiro Belo Dos Santos, S.; Van Tricht, C.; Lammertyn, J.; Spasic, D. Zoonotic disease detection at the point-of-care: the best of RPA and CRISPR-Cas. *Biosens. Bioelectron.* **2025**, *293*, 118139, DOI: 10.1016/j.bios.2025.118139

21. Chen, L.; Hu, M. L.; Zhou, X. M. Trends in developing one-pot CRISPR diagnostics strategies. *Trends Biotechnol.* **2024**, *43* (1), 98-110, DOI: 10.1016/j.tibtech.2024.07.007

22. Hu, W. T.; Zhao, Y.; Qi, H. B.; Sun, H.; Xie, Y. Y.; Wang, Y.; Liang, Q. L. Advances in Point-of-Care Testing (POCT) based on microfluidic chips towards small molecular biomarkers. *Trends Anal. Chem.* **2026**, *195*, 118596, DOI: 10.1016/j.trac.2025.118596

23. Pan, Y. W.; Mao, K.; Hui, Q. X.; Wang, B. J.; Cooper, J.; Yang, Z. G. Paper-based devices for rapid diagnosis and wastewater surveillance. *Trends Anal. Chem.* **2022**, *157*, 116760, DOI: 10.1016/j.trac.2022.116760

24. Yang, Z. Y.; Lou, Y. F.; Sun, L. N.; Chen, S. Y.; Li, M. S.; Lu, Z. X.; Zhang, L. M.; Cao, R.; Tian, J. F. Recent advancements in paper microfluidics for blood analysis and diagnostics. *Trends Anal. Chem.* **2025**, *190*, 118289, DOI: 10.1016/j.trac.2025.118289

25. Pan, Y.; Wang, B.; Cooper, J. M.; Yang, Z. Paper microfluidic sentinel sensors enable rapid and on-site wastewater surveillance in community settings. *Cell Rep. Phys. Sci.* **2024**, *5* (10), 102154, DOI: 10.1016/jxcrp.2024.102154

26. Piwowarska, D.; Kiedrzyńska, E.; Jaszczyszyn, K. J. A global perspective on the nature and fate of heavy metals polluting water ecosystems, and their impact and remediation. *Crit. Rev. Environ. Sci.* **2024**, *54* (19), 1436–1458, DOI: 10.1016/j.trac.2025.118289

27. Yang, N.; Zhang, H.; Han, X.; Liu, Z. F.; Lu, Y. Advancements and applications of loop-mediated isothermal amplification technology: a comprehensive overview. *Front Microbiol.* **2024**, *15*, 1406632, DOI: 10.3389/fmicb.2024.1406632

28. Mukama, O.; Wu, J. H.; Li, Z. Y.; Liang, Q. X.; Yi, Z. J.; Lu, X. W.; Liu, Y. J.; Liu, Y. M.; Hussain, M.; Makafe, G. G.; Liu, J. X.; Xu, N.; Zeng, L. W. An ultrasensitive and specific point-of-care CRISPR/Cas12 based lateral flow biosensor for the rapid detection of nucleic acids. *Biosens. Bioelectron.* **2020**, *159*, 112143, DOI: 10.1016/j.bios.2020.112143

29. Lv, X. R.; Wang, L.; Zhang, J. F.; Zeng, H. Y.; Chen, X.; Shi, L.; Cui, H. L.; He, X. X.; Zhao, L. C. Rapid and sensitive detection of VBNC Escherichia coli O157: H7 in beef by PMAxx and real-time LAMP. *Food Control* **2020**, *115*, 107292, DOI: 10.1016/j.foodcont.2020.107292

30. Hong, J. Development and application of the loop-mediated isothermal amplification assay for rapid detection of enterotoxigenic *Clostridium perfringens* in food. *J. Food Saf.* **2017**, *37*, 7, DOI: 10.1111/jfs.12362

31. Sridapan, T.; Tangkawsakul, W.; Janvilisri, T.; Kiatpathomchai, W.; Dangtip, S.; Ngamwongsatit, N.; Nacapricha, D.; Ounjai, P.; Chankhamhaengdecha, S. Rapid detection of *Clostridium perfringens* in food by loop-mediated isothermal amplification combined with a lateral flow biosensor. *PLoS One* **2021**, *16* (1), e0245144, DOI: 10.1371/journal.pone.0245144

32. Bonetta, S.; Pignata, C.; Lorenzi, E.; De Ceglia, M.; Meucci, L.; Bonetta, S.; Gilli, G.; Carraro, E. Detection of pathogenic *Campylobacter*, *E. coli* O157:H7 and *Salmonella* spp. in wastewater by PCR assay. *Environ. Sci. Pollut. Res.* **2016**, *23* (15), 15302–15309, DOI: 10.1007/s11356-016-6682-5

33. Fuhrimann, S.; Pham-Duc, P.; Cissé, G.; Tram, N. T.; Thu Ha, H.; Dung, D. T.; Ngoc, P.; Nguyen-Viet, H.; Anh Vuong, T.; Utzinger, J.; Schindler, C.; Winkler, M. S. Microbial contamination along the main open wastewater and storm water channel of Hanoi, Vietnam, and potential health risks for urban farmers. *Sci. Total Environ.* **2016**, *566*, 1014–1022, DOI: 10.1016/j.scitotenv.2016.05.080

34. Bonetta, S.; Pignata, C.; Gasparro, E.; Richiardi, L.; Bonetta, S.; Carraro, E. Impact of wastewater treatment plants on microbiological contamination for evaluating the risks of wastewater reuse. *Environ. Sci. Eur.* **2022**, *34*, 20, DOI: 10.1186/s12302-022-00597-0

35. Namadi, P.; Deng, Z. Optimum environmental conditions controlling prevalence of vibrio parahaemolyticus in marine environment. *Mar. Environ. Res.* **2023**, *183*, 105828, DOI: 10.1016/j.marenvres.2022.105828

36. Gómez, P.; Lozano, C.; Benito, D.; Estepa, V.; Tenorio, C.; Zarazaga, M.; Torres, C. Characterization of *staphylococci* in urban wastewater treatment plants in Spain, with detection of methicillin resistant *Staphylococcus aureus* ST398. *Environ. Pollut.* **2016**, *212*, 71–76, DOI: 10.1016/j.envpol.2016.01.038

37. Lass, A.; Kontogeorgos, I.; Ma, L.; Zhang, X.; Li, X.; Karanis, P. Investigation of *Toxoplasma gondii* in wastewater and surface water in the Qinghai-Tibet Plateau, China using real-time PCR and multilocus genotyping. *Sci. Rep.* **2022**, *12* (1), 5428., DOI: 10.1038/s41598-022-09166-0

38. Abia, A.L.K.; Ubomba-Jaswa, E.; du Preez, M.; Momba, M. N. B. Riverbed sediments in the Apies River, South Africa: recommending the use of both *Clostridium perfringens* and *Escherichia coli* as

indicators of faecal pollution. *J. Soils Sediments* **2015**, *15*, 2412–2424, DOI: 10.1007/s11368-015-1209-0

39. Ho, Y. N.,; Tsai, H. C.; Hsu, B. M.; Chiou, C. S. The association of *Salmonella enterica* from aquatic environmental and clinical samples in Taiwan. *Sci. Total Environ.* **2018**, *624*, 106–113, DOI: 10.1016/j.scitotenv.2017.12.122
40. Kayode, A. J.; Semerjian, L.; Osaili, T.; Olapade, O.; Okoh, A. I. Occurrence of multidrug-resistant *listeria monocytogenes* in environmental waters: A menace of environmental and public health concern. *Front. environ. sci.* **2021**, *9*, 737435, DOI: 10.3389/fenvs.2021.737435
41. Stea, E. C.; Purdue, L. M.; Jamieson, R. C.; Yost, C. K.; Truelstrup Hansen, L. Comparison of the prevalences and diversities of *listeria* species and *listeria monocytogenes* in an urban and a rural agricultural watershed. *Appl. Environ. Microbiol.* **2015**, *81*, 3812–3822, DOI: 10.1128/AEM.00416-15
42. Gholipour, S.; Nikaeen, M.; Farhadkhani, M.; Nikmanesh, B. Survey of *Listeria monocytogenes* contamination of various environmental samples and associated health risks. *Food Control* **2020**, *108*, 106843, DOI: 10.1016/j.foodcont.2019.106843
43. Galvani, A. T.; Christ, A. P. G.; Padula, J. A.; Barbosa, M. R. F.; de Araújo, R. S.; Sato, M. I. Z.; Razzolini, M. T. P. Real-time PCR detection of *Toxoplasma gondii* in surface water samples in São Paulo, Brazil. *Parasitol. Res.* **2019**, *118*, 631–640, DOI: 10.1007/s00436-018-6185-z
44. Lv, X. R.; Wang, L.; Zhang, J. F.; Zeng, H. Y.; Chen, X.; Shi, L.; Cui, H. L.; He, X. X.; Zhao, L. C. Holistic one health surveillance framework: Synergizing environmental, animal, and human determinants for enhanced infectious disease management. *ACS Infect Dis.* **2024**, *10* (3), 808–826, DOI: 10.1021/acsinfecdis.3c00625
45. Yin, K.; Ding, X.; Xu, Z. H.; Li, Z. Y.; Wang, X. Y.; Zhao, H.; Otis, C.; Li, B. K.; Liu, C. C. Multiplexed colorimetric detection of SARS-CoV-2 and other pathogens in wastewater on a 3D printed integrated microfluidic chip. *Sens Actuators B Chem.* **2021**, *344*, 130242, DOI: 10.1016/j.snb.2021.130242
46. Xing, G. W.; Shang, Y. T.; Wang, X. R.; Lin, H. F.; Chen, S. L.; Pu, Q. S.; Lin, L. Multiplexed detection of foodborne pathogens using one-pot CRISPR/Cas12a combined with recombinase aided

amplification on a finger-actuated microfluidic biosensor. *Biosens. Bioelectron.* **2023**, *220*, 114885, DOI: 10.1016/j.bios.2022.114885

47. Wei, L. Y.; Wang, Z. L.; Wang, J.; Wang, X. H.; Chen, Y. P. Aptamer-based colorimetric detection of methicillin-resistant Staphylococcus aureus by using a CRISPR/Cas12a system and recombinase polymerase amplification. *Anal. Chim. Acta.* **2022**, *1230*, 340357, DOI: 10.1016/j.aca.2022.340357

48. Wang, W. W.; Zhang, S.; Wang, Y. J.; Ge, J. Y.; Li, L. Metagenomic and cytotoxicity insights into the migration behavior and pathogenic potential of multi-medium microorganisms in a wastewater treatment plant. *Water Res.* **2026**, *292*, 125285, DOI: 10.1016/j.watres.2025.125285

49. Li, J. Y.; Choi, P. M.; Gao, J. F.; Ren, J. N.; O'Brien, J. W.; Thomas, K. V.; Mueller, J. F.; Thai, P. K.; Jiang, G. M. In-sewer stability of 31 human health biomarkers and suitability for wastewater-based epidemiology. *Water Res.* **2024**, *249*, 120978, DOI: 10.1016/j.watres.2023.120978

50. Meadows, T.; Coats, E. R.; Narum, S.; Top, E. M.; Ridenhour, B. J.; Stalder, T. Epidemiological model can forecast COVID-19 outbreaks from wastewater-based surveillance in rural communities. *Water Res.* **2025**, *268*, 122671, DOI: 10.1016/j.watres.2024.122671

51. Stoffers, T.; Altermatt, F.; Baldan, D.; Bilous, O.; Borgwardt, F.; Buijse, A. D.; Bondar-Kunze, E.; Cid, N.; Erős, T.; Ferreira, M. T.; Funk, A. Reviving Europe's rivers: Seven challenges in the implementation of the Nature Restoration Law to restore free-flowing rivers. *Wiley Interdiscip. Rev.: Water* **2024**, *11* (3), e1717, DOI: 10.1002/wat2.1717

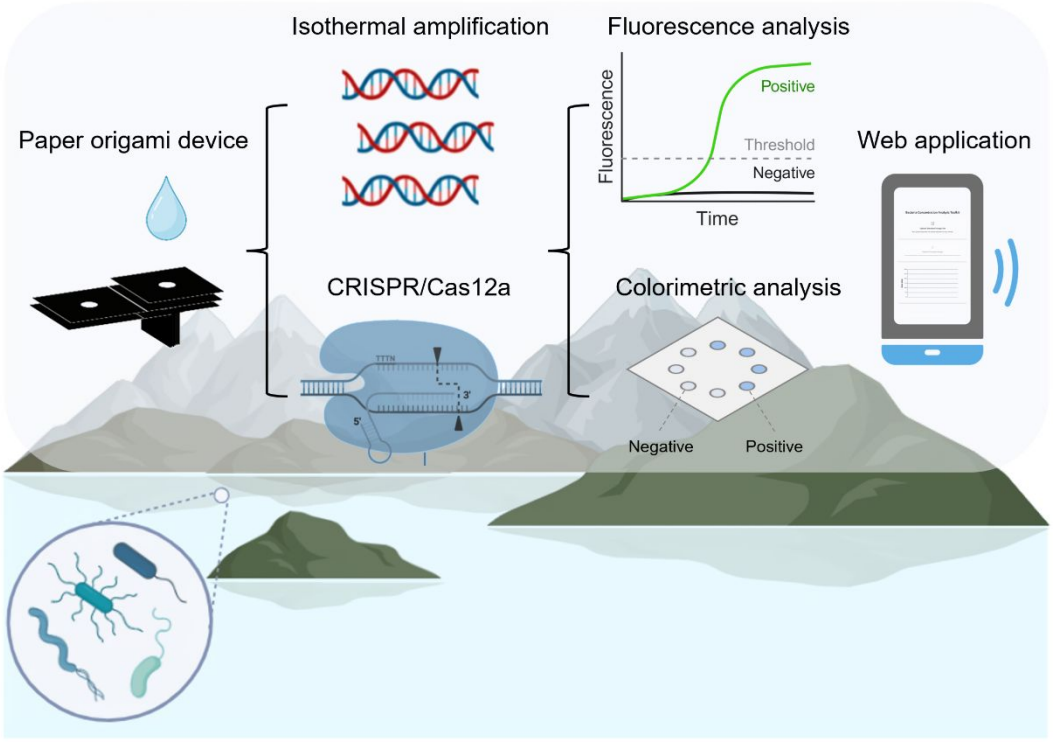
52. Singh, P. K.; Kumar, U.; Kumar, I.; Dwivedi, A.; Singh, P.; Mishra, S.; Seth, C. S.; Sharma, R. K. Critical review on toxic contaminants in surface water ecosystem: sources, monitoring, and its impact on human health. *Environ. Sci. Pollut. Res. Int.* **2024**, *31* (45), DOI: 56428–56462

Table of contents: We developed a paper microfluidic platform for spatially multiplexed pathogen detection in resource-limited settings. The platform combined syringe filtration for rapid sample processing, various paper-based isothermal amplification and CRISPR-Cas detection, solar-powered portable incubation/imaging hardware, and web application for quantitative analysis. The platform achieved single-CFU sensitivity and delivered sample-to-answer results within 60 min, enabling high-throughput, low-cost, and environmentally-friendly field testing. This strategy provided a powerful tool for aquatic monitoring, with significant implications for public health protection and emerging epidemic monitoring.

Yuwei Pan, Zhugen Yang

Paper microfluidic platform using multiplexed isothermal amplification and CRISPR/Cas12a for aquatic pathogen detection

ToC Figure



Figures and Tables

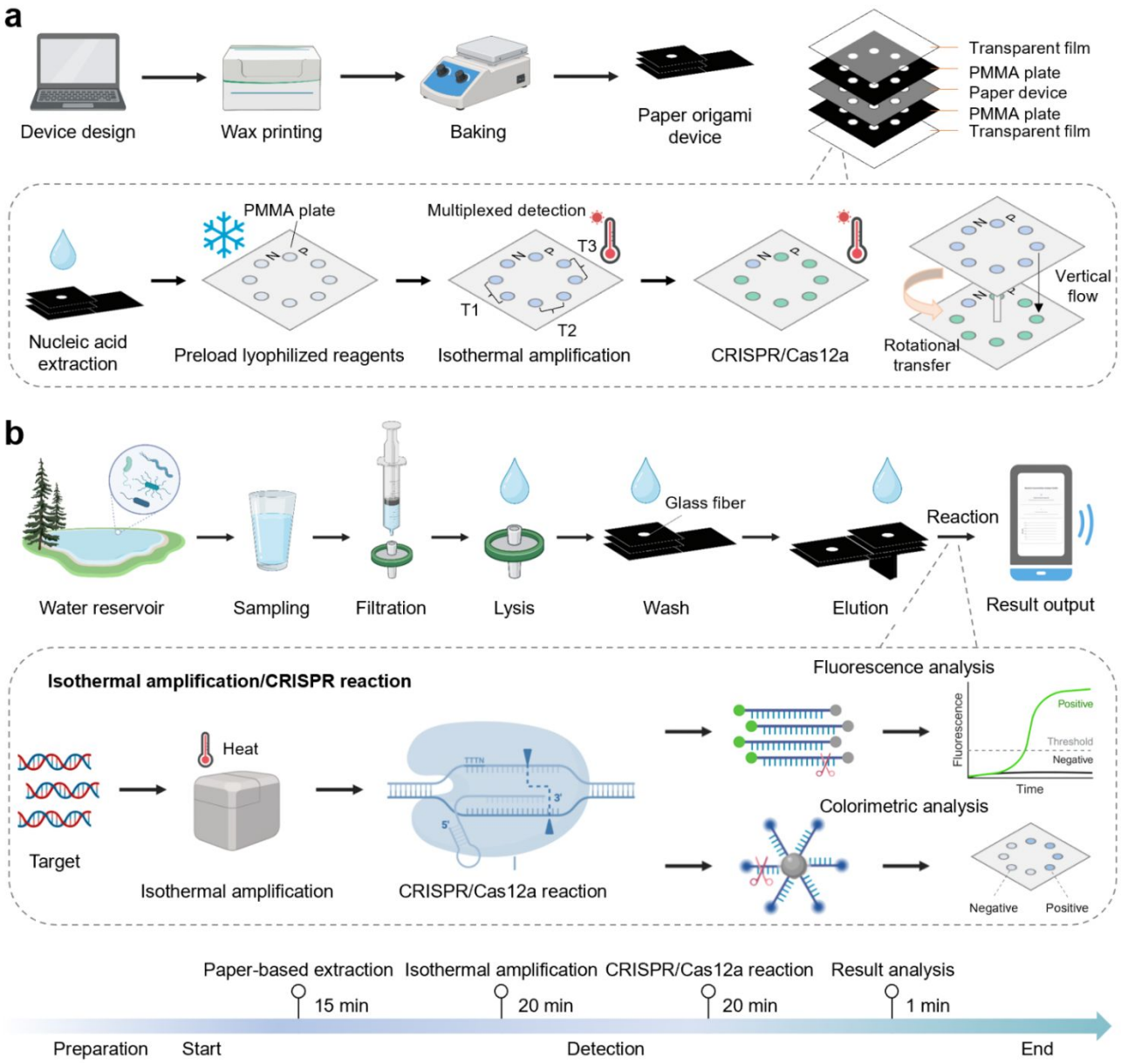


Figure 1. Paper microfluidic platform for aquatic pathogen detection. a, Fabrication workflow. Wax-printed paper origami devices were designed in CorelDraw, patterned, and heat-treated (130 °C for 5 min) before preloading with lyophilized isothermal amplification/CRISPR reagents. The biosensor comprised a paper microfluidic chip with hydrophilic white zones and hydrophobic black barriers, and a laser-cut poly(methyl methacrylate) (PMMA) substrate serving as reaction chambers. Analytical workflow included paper-based nucleic acid extraction, lyophilized reagent storage, isothermal amplification, and CRISPR/Cas12a detection. The dual-layer architecture physically isolated chambers for separate amplification and detection, enabling unidirectional product transfer via rotational alignment. T1, Target 1; T2, Target 2; T3, Target 3. **b,** Analytical workflow. Top panel: Analytical workflow of paper microfluidic biosensor. Water samples were filtered and lysed, with nucleic acids extracted via glass fiber adsorption, followed by ethanol wash/nuclease-free water elution. Punched discs

transferred nucleic acids to reaction chambers containing lyophilized reagents. Results were interpreted either through visual inspection (qualitative) or quantified via mobile phone camera imaging coupled to custom web application. Middle panel: Molecular mechanism showing crRNA-guided Cas12a target recognition activating collateral cleavage of reporter probes (FQ reporters for fluorescence analysis, HRP-ssDNA-MB for colorimetric analysis). Bottom panel: Timeline highlighting on-site isothermal amplification-CRISPR detection.

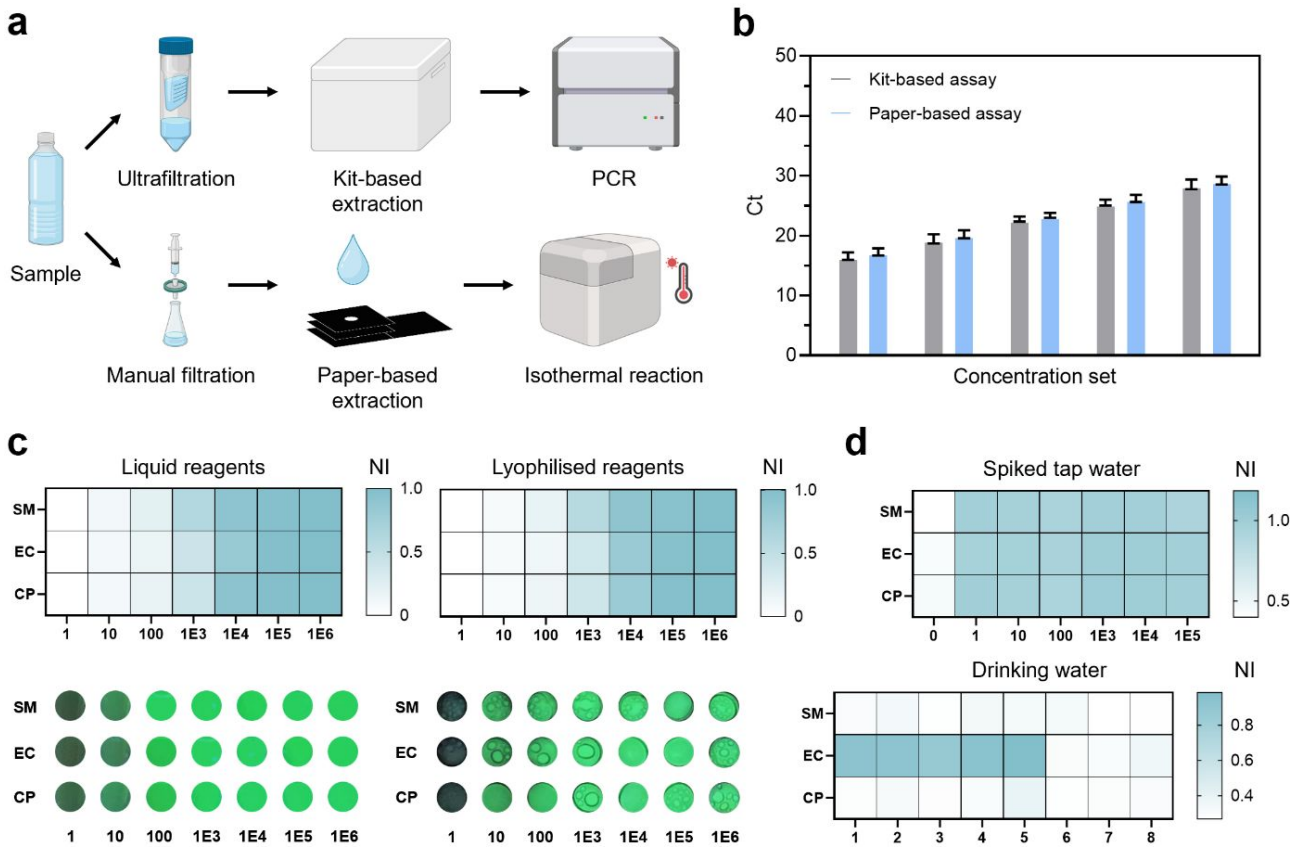


Figure 2. Sample processing and LAMP assay on paper microfluidic biosensor. a, Schematic overview of evaluated enrichment strategies (ultrafiltration vs. manual filtration), nucleic acid extraction methods (commercial kits vs. paper-based), and NAATs (PCR vs. isothermal amplification). **b,** Comparative C_t values between commercial extraction kits and paper-based methods following manual filtration. Data are presented as mean ± SD (n = 3). **c,** Heatmap and representative images of paper-based LAMP performance comparing liquid versus lyophilized reagent formulations. **d,** Heatmap of sensitivity assessment in spiked tap water (0–10^5 CFU/mL) and drinking water matrices.

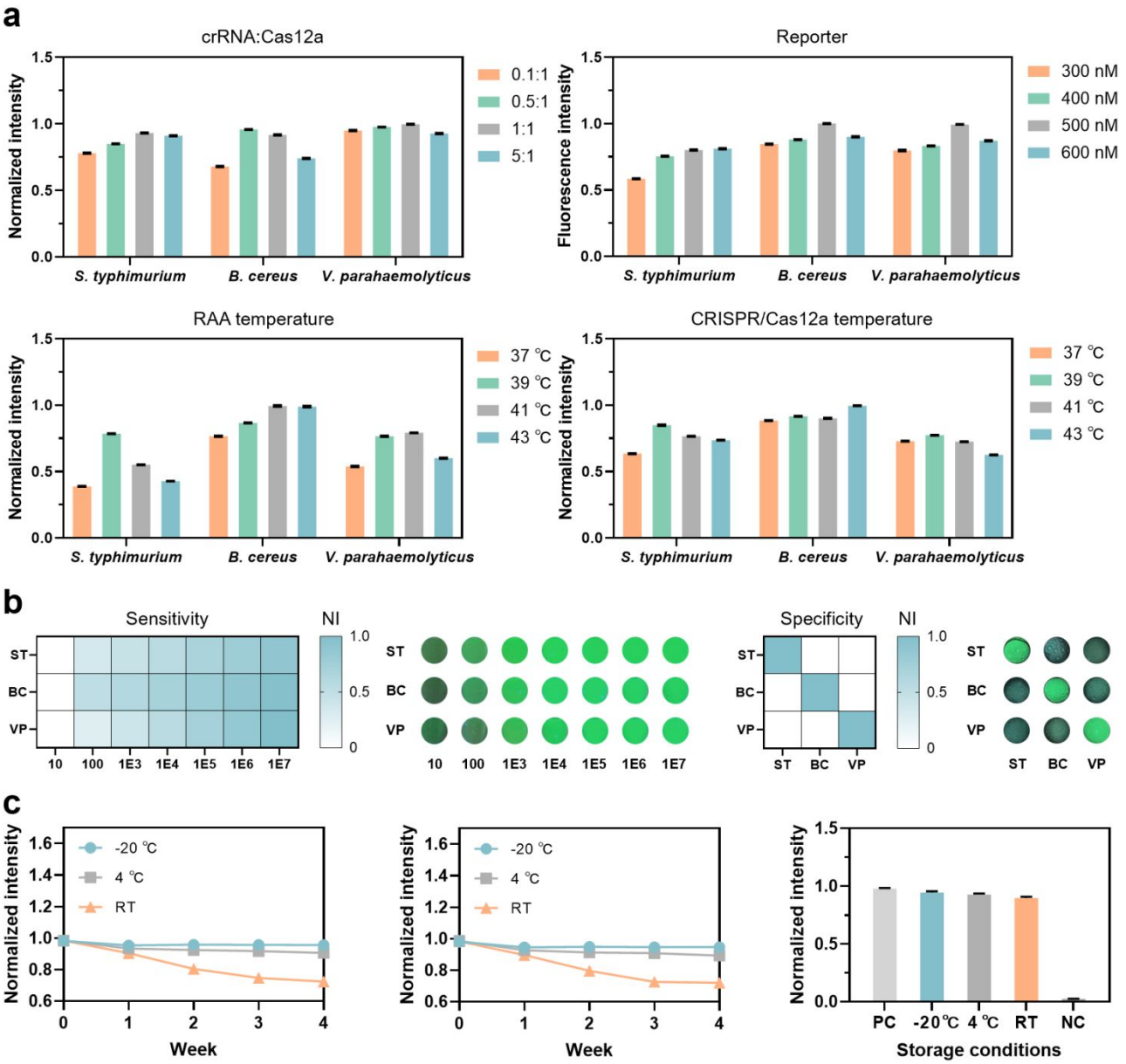


Figure 3. Fluorescent RAA-CRISPR assay on paper microfluidic biosensor. a, Reaction condition optimization. Top left panel: crRNA : Cas12a molar ratios (0.1:1–5:1). Top right panel: ssDNA reporter concentrations (300–600 nM). Bottom left panel: RAA amplification temperatures (37–43 °C). Bottom right panel: Cas12a reaction temperatures (37–43°C). **b**, Analytical performance assessment. Heatmap and representative images demonstrating sensitive and specific detection of *S. typhimurium*, *B. cereus*, and *V. parahaemolyticus* across 10–10^7 CFU/mL. **c,** Lyophilization evaluation. Evaluation of storage conditions for RAA and RAA-CRISPR lyophilized reagents, including fluorescence analysis. RT, room temperature; PC, liquid reagents; NC, nuclease-free water. Data are presented as mean ± SD (n = 3).

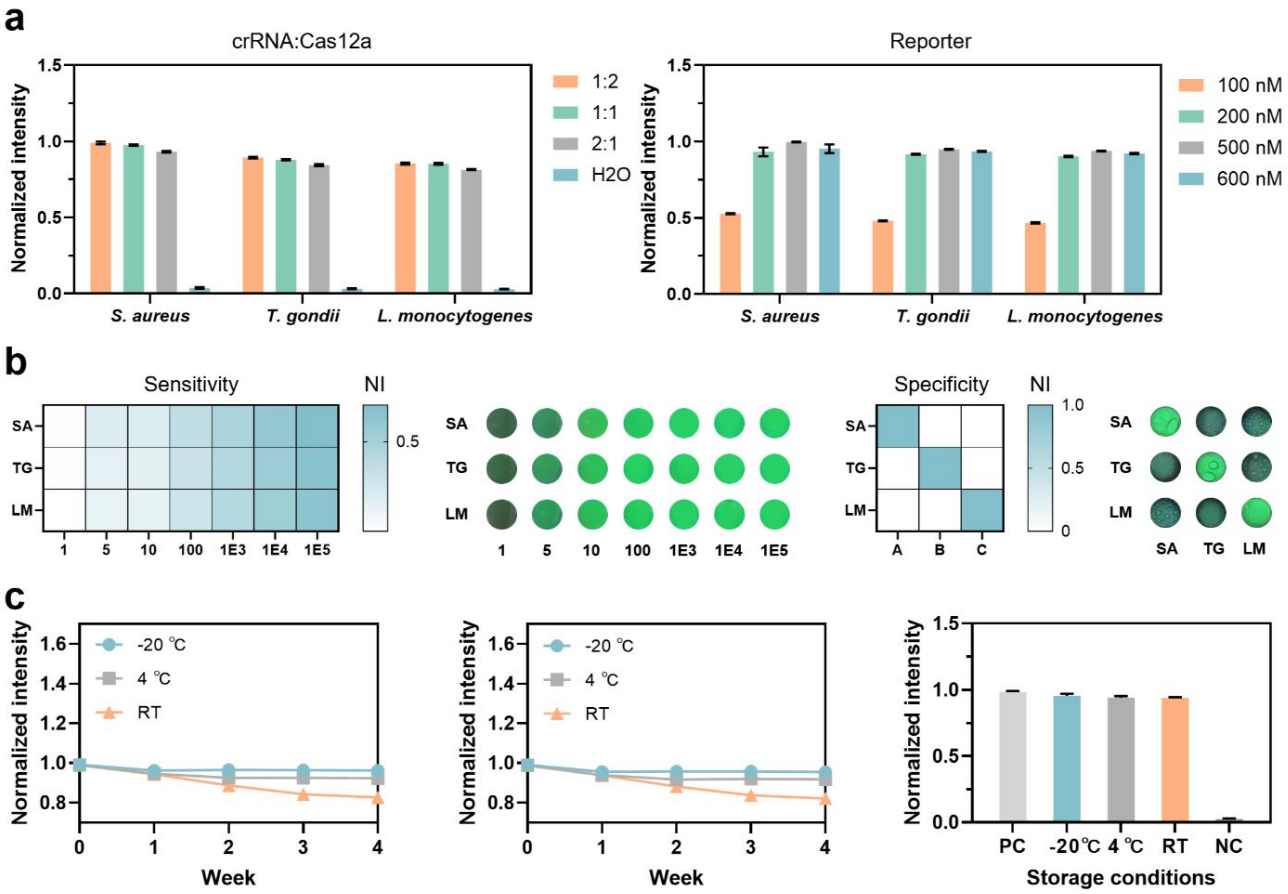


Figure 4. Fluorescent RPA-CRISPR assay on paper microfluidic biosensor. a, Reaction condition optimization. Left panel: crRNA : Cas12a molar ratios (1:2–2:1). Right panel: ssDNA reporter concentrations (100–600 nM). **b**, Analytical performance assessment. Heatmap and representative images demonstrating sensitive and specific detection of *S. aureus*, *T. gondii*, and *L. monocytogenes* across 1–10^5 CFU/mL. **c,** Lyophilization evaluation. Evaluation of storage conditions for RPA and RPA-CRISPR lyophilized reagents, including fluorescence analysis. RT, room temperature; PC, liquid reagents; NC, nuclease-free water. Data are presented as mean ± SD (n = 3).

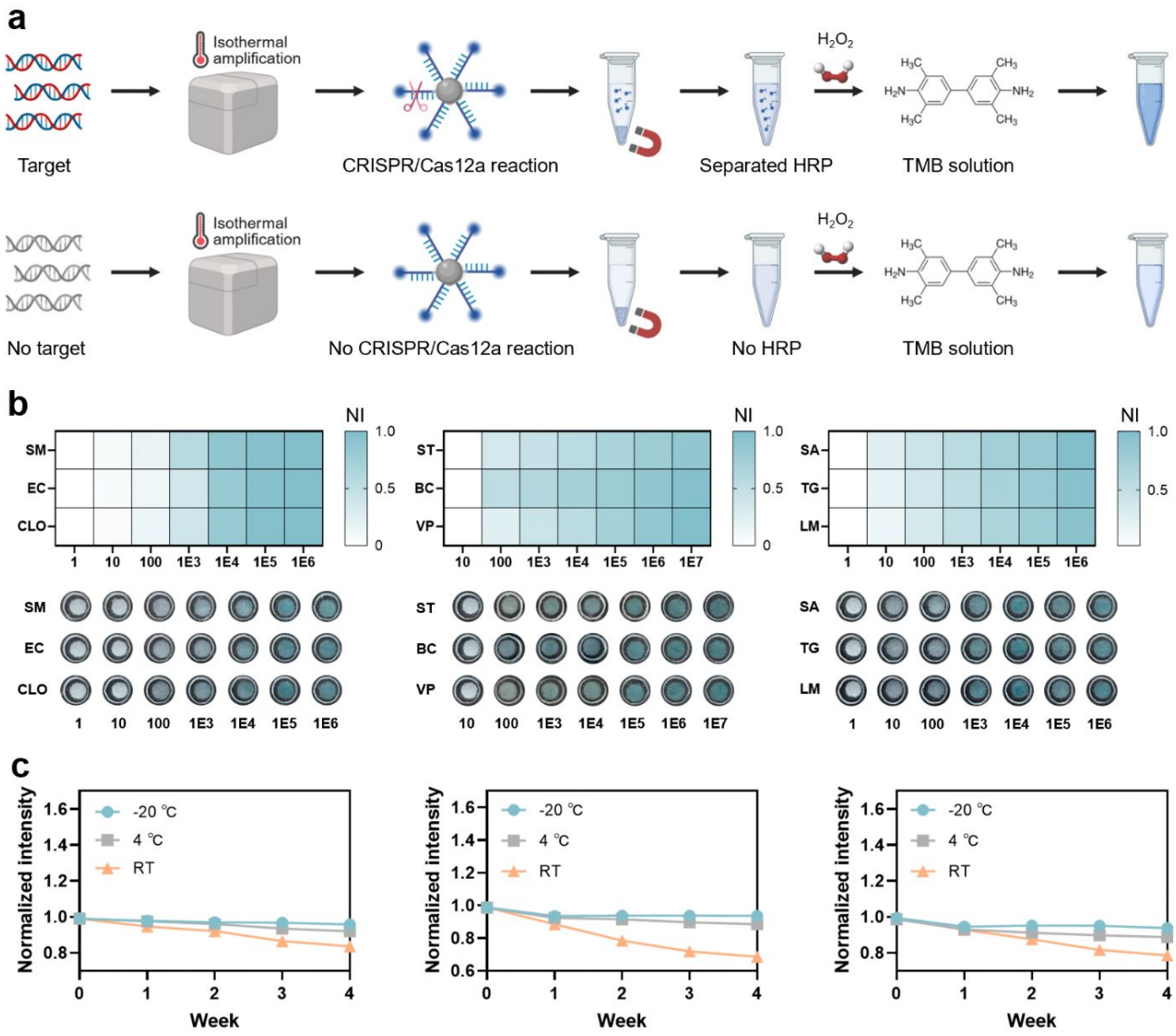


Figure 5. Colorimetric isothermal amplification-CRISPR assay on paper microfluidic biosensor. a, Analytical workflow. Cas12a-crRNA complex recognized target sequence and activated its trans-cleavage activity. This cleaved ssDNA linker and released HRP from MBs. Under magnetic separation, MBs were retained at the bottom, while HRP remained in the supernatant. Transferring the supernatant to TMB solution induced a color change to blue. In the absence of target, Cas12a complex remained inactive and leaved HRP bound to MBs. No HRP entered the supernatant, and TMB solution remained colourless. **b,** Analytical performance assessment. Target bacteria included *Salmonella* (SA), *E. coli* (EC), C. *perfringens* (CP), *S. Typhimurium* (ST), *B. cereus* (BC), *V. parahaemolyticus* (VP), *S. aureus* (SA), *T. gondii* (TG), and *L. monocytogenes* (LM). Heatmap and representative images demonstrating sensitive and specific detection across 1–10^7 CFU/mL. **c,** Lyophilization evaluation. Evaluation of storage conditions for LAMP, RAA-CRISPR, and RPA-CRISPR lyophilized reagents. RT, room temperature; PC, liquid reagents; NC, ddH_2O. Data are presented as mean ± SD (n = 3).

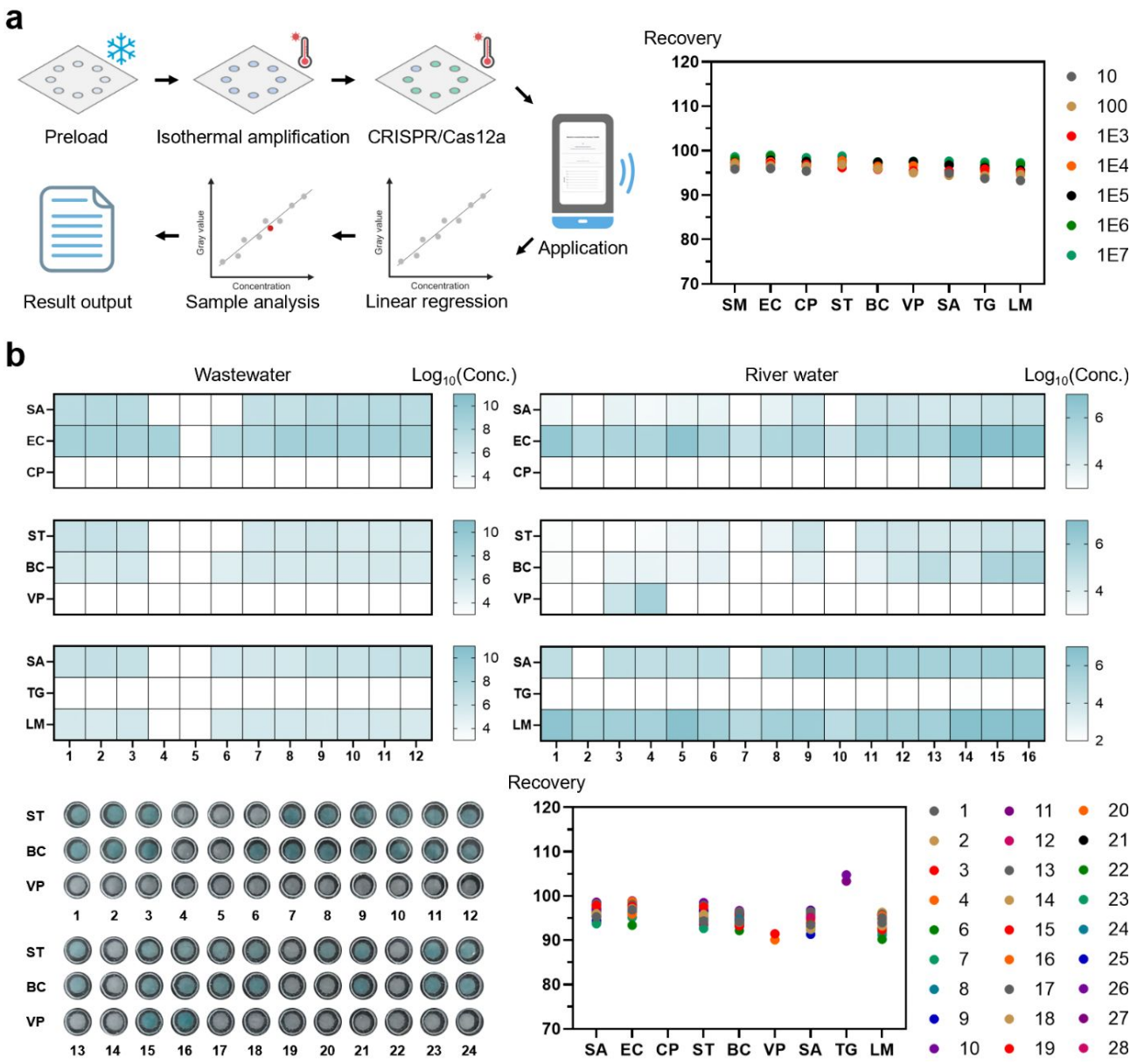


Figure 6. Paper microfluidic platform for on-site pathogen detection in aquatic systems. a, Left panel: Analytical workflow. Field testing was conducted using paper origami devices that were lyophilized and transported with solar-powered portable incubation/imaging hardware via public transit to diverse aquatic systems. Mobile phone-captured images were processed using custom web application. A calibration curve was generated from standard concentrations to correlate grayscale values with bacterial load, and sample grayscale values were converted to concentrations. Right panel: Bacterial recovery in spiked samples, calculated as ratios of software-derived concentrations to PCR-measured values. **b,** Up left panel: Heatmap demonstrating detection across different wastewater matrices (1–12). Up right panel: Heatmap demonstrating detection across different river water matrices from four cities (Edinburgh, 1–4; Glasgow, 5–8; Milton Keynes, 9–12; London, 13–16). Bottom left panel: Representative images. Bottom right panel: Bacterial recovery in wastewater matrices (1–12) and river water

matrices (13–28). Recovery rates were calculated as the ratio of software-derived concentrations to PCR-measured values. Log10(Conc.), Log10(Concentration)(Copies/L).



https://dspace.org/

Paper microfluidic platform using multiplexed isothermal amplification and CRISPR/Cas12a for aquatic pathogen detection

Pan, Yuwei; Yang, Zhugen

2026-12-31
American Chemical Society (ACS)
https://doi.org/10.1021/acssensors.6c00719
Pan Y, Yang Z. (2026) Paper microfluidic platform using multiplexed isothermal amplification and CRISPR/Cas12a for aquatic pathogen detection. ACS Sensors, Available online 7 July 2026

Downloaded from a DSpace repository. https://dspace.org/